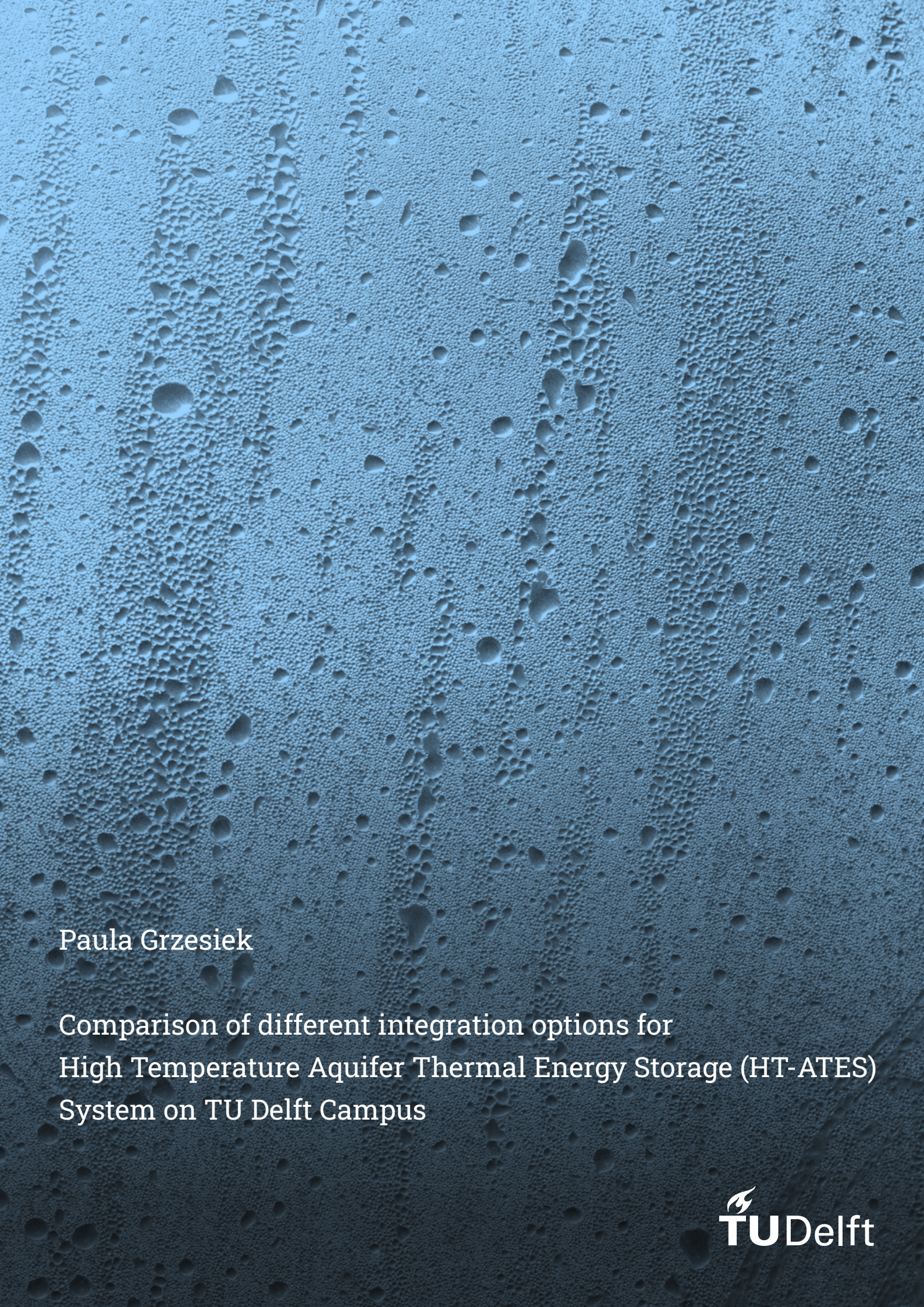

Paula Grzesiek

Comparison of different integration options for High Temperature Aquifer Thermal Energy Storage (HT-ATES) System on TU Delft Campus

TU Delft

Comparison of different integration options for High Temperature Aquifer Thermal Energy Storage (HT-ATES) System on TU Delft Campus

By

Paula Grzesiek

in partial fulfilment of the requirements for the degree of

Master of Science
in Environmental Engineering

at the Delft University of Technology,
to be defended publicly on Thursday August 29, 2024 at 3:00 PM.

Thesis committee:	Dr.ir. J.M. Bloemendal	Committee chair, Main Supervisor
	Prof. Dr. P.J. Vardon	Supervisor
	Ing. L.A. Medema	Supervisor

Abstract

The transition to renewable energy in the heating sector faces significant challenges, particularly the mismatch between the availability of renewable thermal energy sources and fluctuating demand. High Temperature Aquifer Thermal Energy Storage (HT-ATES) systems offer a promising solution to mitigate this mismatch and further decarbonize heating systems by bridging the gap between supply and demand.

This thesis explores the integration of HT-ATES into the heating system at TU Delft, which is transitioning from gas-fired boilers and a combined heat and power plant to a geothermal well-based thermal energy system. During periods of low demand in summer, excess geothermal energy will be stored in the HT-ATES system, to be utilized during high-demand periods in winter when the geothermal well's capacity is exceeded. The objective is to meet 85% of the annual heating demand through sustainable thermal energy sources.

In this study, two design options for integrating the HT-ATES into the heating system are analyzed. Besides the geothermal well and the HT-ATES, the heating system also comprises a heat pump to reach the required supply temperatures. One option is to locate the HT-ATES behind the evaporator of the heat pump and therefore use the previously cooled down temperature to extract thermal energy from the HT-ATES. In the second option, the HT-ATES is located directly behind the heat sink in the system, using the return temperature of the consumers to discharge the HT-ATES.

An energy system model is set up using TESPy and coupled to a numerical model to simulate temperature changes in the HT-ATES. With the results of the model, the influence of the integration concept on the system performance is explained. Furthermore, the effect of varying input parameters such as supply and return temperatures as well as overall demands in the system are examined.

The results indicate that, when comparing the two design options with HT-ATES, locating the HT-ATES behind the evaporator yields the better results across all evaluated performance indicators – mainly a reduction of GHG emissions, an improved system SCOP and a better thermal recovery efficiency of the HT-ATES. However, compared to a base design without HT-ATES, the integration of a HT-ATES leads to additional financial costs and a substantial intervention into the subsurface. Due to its lowest electricity consumption, the base design also shows the best system SCOP.

Acknowledgement

I would like to thank my thesis committee for their availability and support during the completion of this thesis: To Martin Bloemendal for making me curious about ATES systems, a topic that was entirely new to me when starting the thesis. Thanks for our weekly meetings and input on how to model such a system. To Phil Vardon, your positive feedback was always a much-needed motivation boost. It encouraged me to stick to it and reconsider even challenging aspects. To Anne Medema, who provided me with all the details that I needed to know about the system on campus. Your knowledge of the network was the most helpful to get started with my model.

Content

List of Figures

List of Tables

Acronyms

CAPEX	Capital expenditure
CHP	Combined Heat and Power Plant
COP	Coefficient of Performance
GHG	Green House Gas
CHP	Combined Heat and Power
GTD	GeoThermie Delft (Company operating geothermal well)
HT-ATES	High Temperature Aquifer Thermal Energy Storage
OPEX	Operational expenditure
OWD	Open Warmtenet Delft (Company operating heat network to the city of Delft
PI	Performance Indicator
P&ID	Piping and Instrumentation Diagram
$SCOP_{HP}$	Seasonal Coefficient of Performance for the heat pump
$SCOP_{System}$	Seasonal Coefficient of Performance for the system
TUD	Delft University of Technology
WKC	Warmtekrachtcentrale (Buildings in which boilers and CHP are located)

Nomenclature

E_{in}	Injected thermal energy	J
E_{out}	Extracted thermal energy	J
η_s	Isentropic efficiency	-
η_{th}	Thermal recovery efficiency of an ATES	-
h	Enthalpy	J/kg
$\dot{m}$	Mass flow	kg/s
Q	Thermal energy	J
$\dot{Q}$	Thermal output	W
T_C	Temperature cold reservoir	K
T_H	Temperature hot reservoir	K
W	Work	J
$\dot{W}$	Power	W

1 Introduction

The EU has committed itself to reduce greenhouse gas emissions (GHG) by 55% until 2030 compared to 1990. Until today, it has reached a reduction of about 32% (European Commission, 2024) and it is likely that the climate goal will be missed. Heat and electricity in the buildings sector account for 35% of the energy-related emissions in the EU (European Environment Agency, 2023). Decarbonizing the heating sector is thus crucial to meet the target. Although the share of renewable energy in the heating and cooling sector has reached approximately 23% (Eurostat, 2023), the biggest challenge still lies in the mismatch between availability and demand of thermal energy.

The storage of thermal energy in aquifers has emerged as a promising and innovative solution to balance the ever-fluctuating demands and availability of thermal energy. In the Netherlands, over 2 700 such aquifer thermal energy storage (ATES) systems are already installed. An ATES consists of a pair of wells drilled into an underground aquifer, one to inject heat when there is a surplus in heat production and one to extract heat during high demand. Established systems usually store temperatures up to about 25°C (Bloemendal et al., 2020).

Currently, the integration of a high temperature aquifer thermal energy storage (HT-ATES) into the heat supply system of TU Delft (TUD) and Delft city is planned. The HT-ATES will store heat from a geothermal well (GTD well) that has been built on the campus of the university. The GTD well will produce thermal energy at approximately 75°C. The aquifer storage consequently has to store heat at a similar temperature level. Such HT-ATES systems are currently being researched and are not yet a ‘proven technology’ (Zwamborn, 2021). Compared to low temperature ATES, it allows for more energy storage per cubic meter, which reduces the volume that is needed to cover the heat demand of the connected system. The adoption of HT-ATES promises to improve the flexibility of heat supply systems, with a wider range of application, less space needed and reduced need for supplementary heating during peak demands (Drijver et al., 2019).

However, in the case of the heating system on campus, the needed supply temperatures reach up to 90°C due to older buildings of the university. With the GTD well producing about 75°C, a heat pump still needs to be included in the system. The exact integration concept of the heat pump and the HT-ATES within the system is not yet defined and highly depends on the interaction between the two components. The size and operation of the heat pump will influence the proportion of thermal energy that can be used from the HT-ATES. Therefore, different design options for integration of the heat pump and HT-ATES on TUD’s campus emerge.

To objectively compare different design options, an evaluation based on performance indicators (PIs) is required. In literature, the focus often lies on assessing (HT)-ATES systems independently, rather than evaluating the entire heating system in which the HT-ATES is integrated. For example, Drijver et al. (2019) conclude that an ATES system is more efficient, the lower the cut-off temperature is. This is the lowest temperature that can be used from the storage. Stemmle et al. (2021) identify the ATES capacity, flow rate and operating time as the most influencing parameters to reduce electricity consumption and GHG emissions. Fleuchaus et al. (2020) state that performance of ATES systems should be based on recovery rate (how much of the thermal energy injected in the aquifer is recovered), sustainability (efficient use of available subsurface space) and economic efficiency (avoid oversizing of the system).

However, most of these parameters highly depend on the rest of the system in which the ATES is integrated. Gao et al. (2017) show that most studies do not take into account the energy profile of the end users and assume constant injection and extraction flow rates to assess system performance of an ATES system. In reality, however, the injected and extracted volume are rarely equal and also fluctuate over the years. As a result, thermal recovery efficiency is typically lower than in an ideally balanced system. Also, when evaluating GHG emissions and electricity consumption, the full system must be considered. Increasing the thermal output of the GTD well, for example, will lead to a reduction in boiler capacity and thus in GHG emissions. At the same time, the electricity consumption to operate the GTD well will increase. The thermal energy in the system is transferred through a fluid. Always maintaining the mass and energy balance means that increasing the output of one component by adjusting the flow in one part of the system, will affect the flows and temperatures in other connections of the system. These coupled dependencies make the system complex to evaluate and operate. Finally, the importance of considering the full system also becomes apparent when evaluating financial performance. For the system on TUD's campus, the thermal energy produced by the GTD well is subsidized (Bloemendal et al., 2021). This means it is financially interesting to produce as much heat as possible from the GTD well, even if it results in a low thermal recovery efficiency of the HT-ATES.

Another aspect specifically relevant for the case of TUD is the robustness of the system. A reduction in the heat demand of TUD is predicted for the coming years due to improved building efficiency. On the other hand, the heat demand of the city Delft will increase as more and more buildings should be connected to the heating grid in the future. Also, regarding the supply and return temperatures, the currently available data is associated with uncertainties. Efforts to reduce the return and supply temperatures in future are being made which will also affect the flows in the system. The HT-ATES system thus has to be designed to accommodate a wide variety in demands and temperatures.

Research Objective

Regarding the integration of a HT-ATES system to store thermal energy produced by the GTD well on TU Delft campus, different options are being considered. The aim of the thesis is to compare these options based on PIs such as GHG emissions, the seasonal coefficient of performance of the system and thermal recovery efficiency of the HT-ATES. To analyze the interaction between the different components of the system – mainly GTD well, HT-ATES, heat pump and boiler – a deterministic model is developed. Using this model, the following research objectives are addressed:

- Investigate how the integration concept of the HT-ATES within the system influences overall performance.
- Assess the effect of the heat pump size on storage requirement and overall performance.
- Analyze the robustness of the system concerning variations in heat demand, supply and return temperatures.
- Investigate how changes in the merit order of the heat sources (GTD well and HT-ATES) affect the system.
- Compare heat losses and pumping costs for different HT-ATES loading strategies.

2 Methodology

In the following chapter, the concept of the heat network including the GTD well and the HT-ATES is briefly introduced and an overview on the data for the demands and temperatures in the network is given. Then, the setup of the model including the governing equations for the different components as well as the parametrization of the model is explained. The different design options to be analyzed are introduced in section 2.3 followed by an explanation on the sensitivity analysis performed later. For an objective evaluation of the model results, the performance indicators used in this study are presented at the end of the chapter.

2.1 Case Description

Currently, the heating network of TUD is supplied with heat from gas-fired boilers and a combined heat and power plant (CHP). For a more sustainable thermal energy supply, a geothermal well was drilled that will produce heat at a temperature of approximately 75°C. The drilling of the GTD well to a depth of 2200 m was completed in the end of 2023 (*Geothermie Delft*, 2024). The GTD well will be connected not only to the heating network of TUD but also to the district heating of the city of Delft called Open Warmtenet Delft (OWD). In wintertime, the heat demand of OWD and TUD will exceed the capacity of the GTD well. Conversely, during the summertime, the heat demand is significantly lower than what the GTD can provide. To bridge this discrepancy, a HT-ATES will be installed on the campus of the university. The HT-ATES will store heat from the GTD well at a depth of approximately 150 m below the subsurface. At present, pilot drilling is underway to determine the exact location and design of the HT-ATES. The supply temperatures for TUD and OWD vary over the year and depend on the outside air temperatures. At very low outside air temperatures, TUD and OWD will require supply temperatures above the temperature level provided by GTD and HT-ATES. Therefore, a heat pump will be installed between the heat sources and the consumers. For peak demands, gas-fired boilers are still needed. The basic set-up of the network is shown in Figure 1. The HT-ATES system on campus is also part of PUSH-IT project of the EU and will be used as a demonstration site for education and research (*PUSH-IT*, 2024).

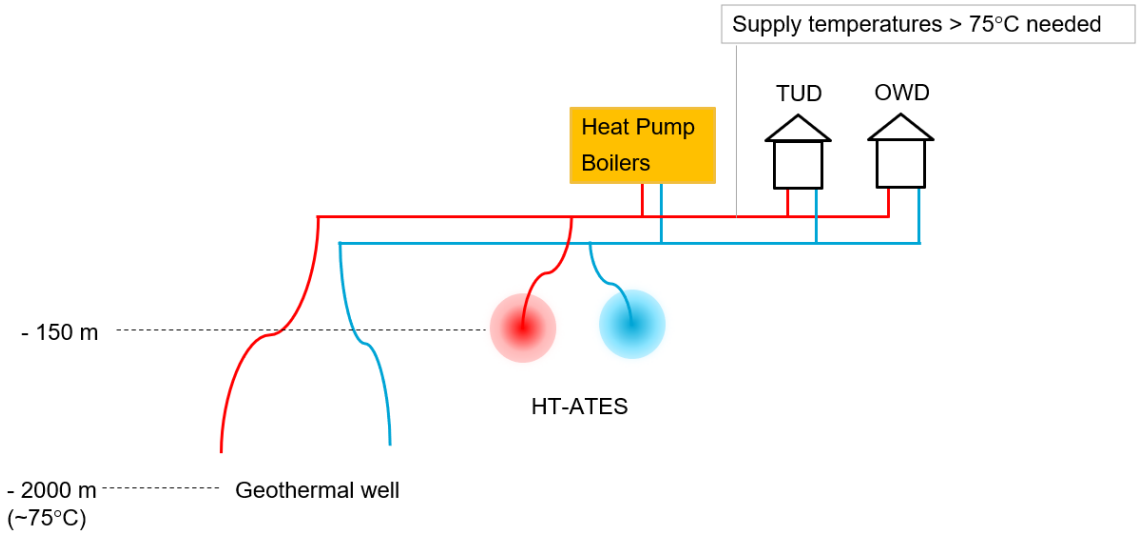

Figure 1 Core concept of the planned heat network on TU Delft Campus (adapted from Bloemendal, 2023)

The system is designed to meet the heat demand of the consumers. The heat demand only refers to heating, domestic hot water consumption is not considered. A complete dataset

containing hourly demand data for TUD and OWD was prepared as an input for the model (see Appendix A). Apart from the heat demands, the dataset also includes the supply and return temperatures for TUD and OWD. The data is shown in Figure 2 and Figure 3. At peak demands, the system will have to supply about 40 MW for both TUD and OWD together. The total annual thermal energy needed in the system is about 92 450 MWh.

Especially for cold outside air temperatures, TUD has slightly higher supply and return temperatures than the OWD network because of older buildings of TUD that are not well insulated. In summertime however, the OWD network needs higher supply and return temperatures than TUD. This is due to bypasses in the OWD network to maintain the needed supply temperatures even for low demands. However, all supply and return temperatures are based on modeled data and are expected to be lower in future due to renovation of the buildings. Also, demands and temperatures for heating purposes only are considered here. It is planned to supply domestic hot water for the OWD network in future, which will again change the demands and temperatures.

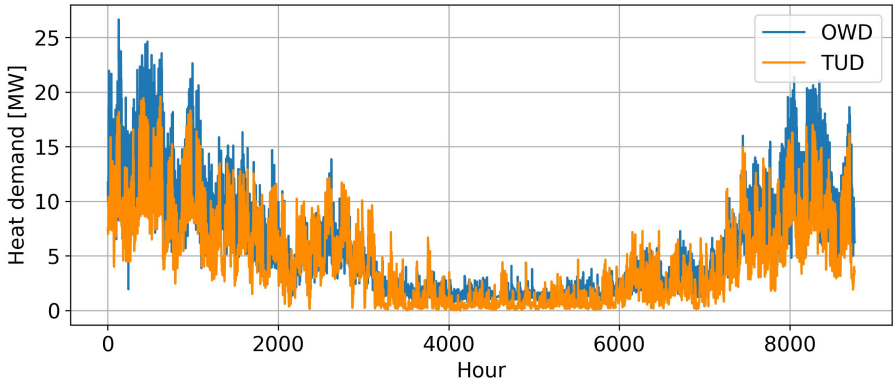

Figure 2 Modeled heat demand for TUD and OWD over one year (from author)

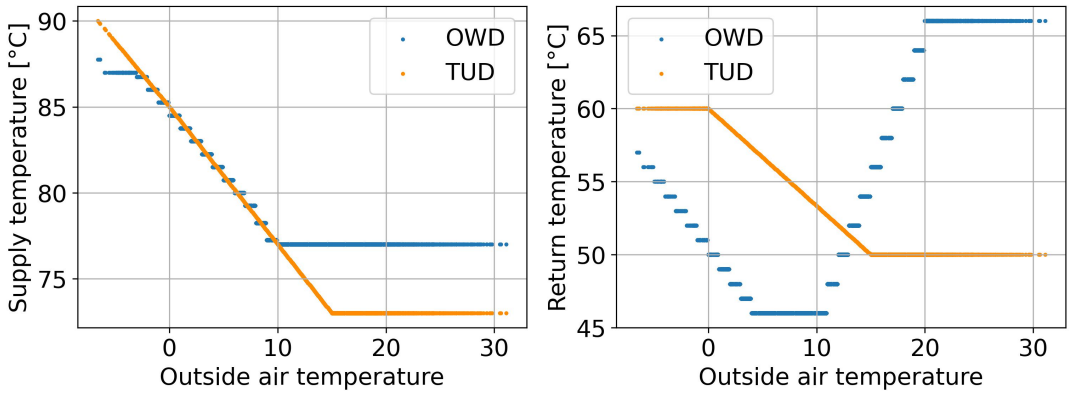

Figure 3 Supply and return temperatures for TUD and OWD depending on outside air temperature (from author)

2.2 Model

HT-ATES and heating systems in general are based on the transferring of heat through a heated fluid. Therefore, the interactions between the system components are described through hydraulic and heat transfer equations. Mass and energy balance are governing the overall behavior of the system. A deterministic model with fixed relationships between the components was developed. Although deterministic models do not account for uncertainties in the system, it is assumed a sufficient approach for the design stage of the system.

The model consists of an energy system model representing the consumers, the heat pump, the GTD well and the boilers in the system and a HT-ATES model simulating the changes in temperature and volume of the HT-ATES. For the energy system model, the open-source python package TESPy was used (Witte & Tuschy, 2020). The energy system model was then coupled with PySeaWATES (Bloemendal, 2024), a numerical model based on MODFLOW (Langevin et al., 2017) to simulate the temperature changes in the aquifer considering complex processes in the subsurface such as heat losses due to buoyancy flow.

Figure 4 illustrates the overall concept of the model: The hourly data for demands, supply and return temperatures of TUD and OWD is used as input for the energy system model. The energy system model solves the energy and mass balance equations for every hour of the year and thus computes the flows and temperatures for loading and discharging the HT-ATES. The flow and temperature that is injected into the HT-ATES (into the hot well when loading and into the cold well when discharging) is handed over to the HT-ATES model. To reduce the computational time, the HT-ATES model is not solved hourly but daily. Therefore, the sum of the injected flow for 24 hours and the average injection temperature for one day is used as an input for the HT-ATES model. If the HT-ATES switches between charging (positive flow) and discharging (negative flow) within the 24 hours in the energy system model, the net total flow for the day is computed and handed over to the HT-ATES model. The numerical HT-ATES model then updates the temperatures of the hot and cold well and again passes on this information to the energy system model. The output data that is generated includes flow rates and temperatures in every connection of the energy system model. Furthermore, the most relevant data retrieved from the model is the thermal output for the GTD well, the HT-ATES, the heat pump and the WKC, as well as the electrical energy consumed by the compressor. Finally, the temperatures in the hot well and the cold well of the HT-ATES are recorded.

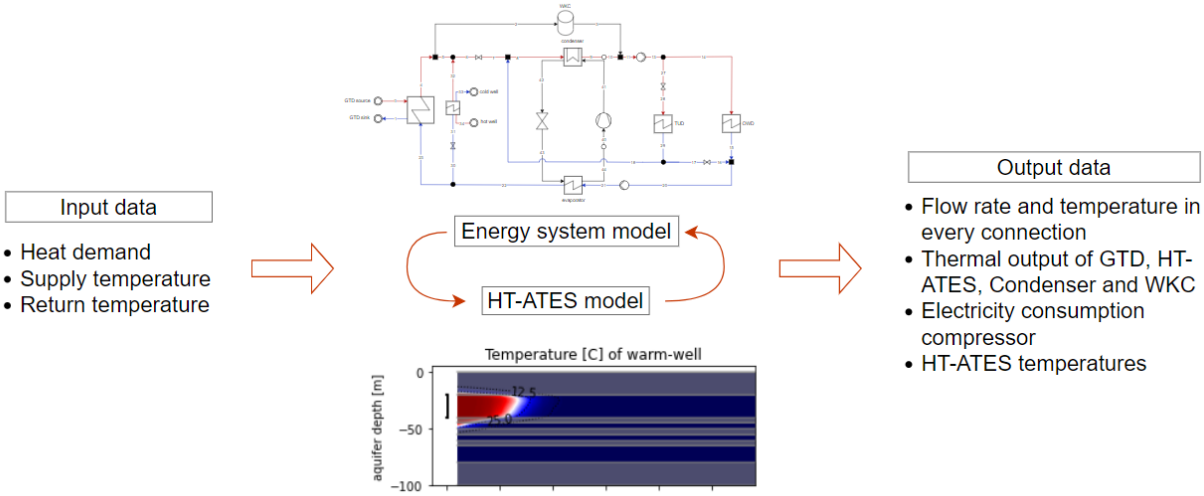

Figure 4 Schematic of the coupled energy system and HT-ATES model

2.2.1 Energy System Model in TESPy

TESPy provides prebuilt components such as heat exchangers, valves, compressors and pipes that can be connected individually. After setting parameters to each component, TESPy generates a linear set of equations to solve for mass flow, pressure, enthalpy and fluid

composition in every connection in the system. The energy balance in the system is defined by the following equation (Witte & Tuschy, 2020):

$$0 = \sum_{o} \dot{m}_{out,o} \cdot h_{out,o} - \sum_{o} \dot{m}_{in,i} \cdot h_{in,i} - \dot{W} - \dot{Q} \quad (1)$$

where $\dot{m}$ is the mass flow in kg/s, h the enthalpy in J/kg, $\dot{W}$ the electrical and mechanical power in Watt and $\dot{Q}$ the thermal output in Watt. The index *o* describes all flows leaving the system and the index *i* all entering connections.

The energy balance is maintained for the overall system and equally for each individual component. The transferred power and heat flux as well as the number of ingoing and outgoing connections depend on a component's characteristics. The following describes the components that are included in the energy system model. For more detailed information, see the official TESPy documentation (Witte, 2024).

Heat Exchangers

As no mechanical or electrical work is transferred in a heat exchanger, the power $\dot{W}$ is equal to 0. Because of mass balance, the mass flow on the inlet and outlet of each side of the heat exchanger has to be equal. In Figure 5 this means that the mass flow in in_1 and out_1 is the same, and the mass flow in in_2 and out_2 is the same. As the thermal output is transferred from the hot side to the cold side of the heat exchanger, the energy balance equation is simplified to (Witte, 2024):

$$0 = \dot{m}_{in,1} \cdot \left(h_{out,1} - h_{in,1}\right) + \dot{m}_{in,2} \cdot \left(h_{out,2} - h_{in,2}\right) \quad (2)$$

The transferred thermal output is defined as (Witte, 2024):

$$\dot{Q} = \dot{m}_{in,1} \cdot \left(h_{out,1} - h_{in,1}\right) \quad (3)$$

For the energy system model in this study, heat exchangers are used to simulate the heat transferred from the GTD well and the HT-ATES into the heating network. In general, the flows on both sides of a heat exchanger are equal and a temperature difference of 1°C is implemented as a heat loss between the hot side and the cold side. In Figure 5 for example, this means that out_2 will be 1°C colder than in_1, and out_1 1°C warmer than in_2. The flow rate in in_1 and in_2 will be the same.

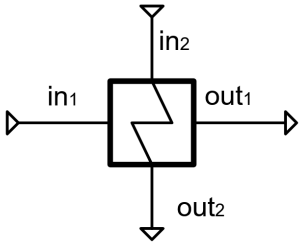

Figure 5 Schematic of a heat exchanger with a hot side (index 1) and a cold side (index 2) (Witte, 2024)

Simplified Heat Exchangers

In TESPy, a heat source or a heat sink can be simulated using a simplified heat exchanger. In this case the cold side of a heat exchanger is ignored (in_2 and out_2 in Figure 5) and only equation (3) is used for the energy balance. The consumers OWD and TUD and the boiler are modeled as simple heat exchangers in this study.

Heat Pump

The heat pump in the model consists of an evaporator, a condenser, a compressor and an expansion valve. The evaporator is modeled using the component heat exchanger as described above. The condenser is a separate component similar to a heat exchanger with an added equation on the hot side to ensure a fully saturated state of the liquid at the outlet. To model the compressor, the isentropic efficiency η_s is set. With this, the energy balance for the compressor is defined as (Witte, 2024):

$$0 = -(h_{out} - h_{in}) \cdot \eta_s + \left(h_{out,s} - h_{in}\right) \tag{4}$$

where $h_{out,s}$ is the enthalpy in J/kg at the outlet if the process were isentropic. In TESPy the isentropic enthalpy is computed using the library CoolProp (Bell et al., 2014). Finally, the expansion valve in the heat pump is a component that reduces the pressure between the inlet and the outlet of the valve without changing the mass flow or enthalpy.

Sinks and Sources

To model the hot and cold well of the HT-ATES and the GTD well, the TESPy components sink and source were used. Sinks and sources do not produce or destroy energy. They enable a flow coming from a source and drain into a sink. The flow from the GTD well originates from a source and drains into a sink after transferring the heat in the heat exchanger. For the HT-ATES, the cold well is a source when loading the HT-ATES and becomes a sink when discharging it (see Figure 6). The hot well on the other side is a source during discharging mode and becomes a sink when loading the HT-ATES.

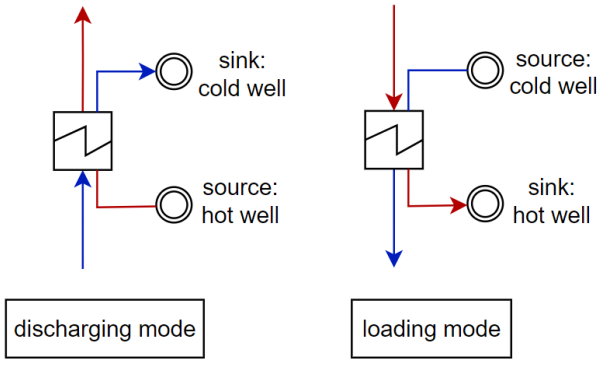

Figure 6 Schematic of discharging and loading mode of the HT-ATES in TESPy (from author)

Basic Components

To ensure a working model, circulation pumps, pressure reducing valves and manifolds were added to the system. As TESPy computes the pressure in every connection, pumps and valves are needed to ensure that the model can be solved. However, pressure losses due to

friction were neglected. The connections between the components were modeled as ideal pipes without friction coefficients. Therefore, the computed power consumption of the circulation pumps in TESPy is not used in the evaluation of the system. As will be explained in section 2.5, the circulation pumps of the GTD well and HT-ATES are analyzed based on a simplified curve function for the power consumption per flow rate.

To include manifolds, TESPy has the pre-built components ‘merges’ and ‘splitters’. These are nodes with multiple inflows or outflows respectively. In the case of the system modeled in this study, flows can change directions and therefore the same node is sometimes a splitter and sometimes a merge. In TESPy, the flow direction can be negative. However, to ensure that the mixing temperature of merging or splitting flows is correctly computed, all inflows into a merge have to be positive as well as all outflows from a splitter. Therefore, the model is set up in a way, that splitters and merges can be interchanged, to always ensure correct mixing temperatures. Solving one mode therefore sometimes requires iteration until all nodes are adjusted correctly.

2.2.2 HT-ATES model in PySeawATES

PySeawATES is a python code to numerically model an aquifer thermal energy storage using MODFLOW, MT3DMS and SEAWAT. MODFLOW is a widely used software to model groundwater flows and MT3DMS simulates solute transport representing the processes of advection, dispersion and chemical reactions between solutes. SEAWAT extends these capabilities and incorporates the possibility to model heat transport in the subsurface using the mathematical analogies between heat transport and solute transport (Langevin et al., 2008). Based on this software, PySeawATES allows for simple adaptation to the specific ATES to be analyzed. An Excel file in which layer and well properties of the ATES can be adjusted serves as the input file for PySeawATES.

For the numerical simulation it is possible to choose between a 3D model and an axisymmetric model. While 3D models are indispensable to investigate complex issues such as the interference of the hot and cold well of an ATES system, an axisymmetric model can enormously improve the computational time by reducing the model by one dimension (Langevin, 2008). As ATES systems inject and extract groundwater through wells, a radial symmetry can be assumed for the groundwater flows around the well. Therefore, it was chosen to use the axisymmetric option in PySeawATES.

Furthermore, the ATES can be modeled using a linear or a logarithmic grid spacing. Due to the finer grid resolution near the wells, logarithmic modeling can better capture steep temperature gradients. In the present case study, linear grid spacing was chosen as the focus lies on the average temperature in the HT-ATES and the total volume of the groundwater storage.

2.2.3 Model Parametrization

Parametrization in PySeawATES

To model the temperature changes in the HT-ATES as accurate as possible, parameters for the subsurface have to be set in PySeawATES. The aquifer in which the HT-ATES will be installed lies at a depth of 120 to 182 meters within the Maassluis formation. The geohydrological conditions of the aquifer highly influence the heat losses of the aquifer storage. Especially the thickness and depth of the aquifer as well as the vertical and

horizontal hydraulic conductivity affect the shape of the thermal plume and therefore the contact surface with the surrounding groundwater causing heat losses (Bloemendal et al., 2020). The aquifer layer properties used in the simulation are based on preliminary results from well test (see Table 11 in Appendix C). Within the aquifer, the well screen was set at a depth range of - 20m to - 40m depth which is only the first unconfined layer of the aquifer. An alternative approach would be to extend the screen length to the full aquifer thickness. However, this would complicate the simulation as the confining layers within the HT-ATES would have to be considered. While an HT-ATES can consist of multiple hot and cold wells, this study focused on a simplified configuration with only one hot well and one cold well.

During the first year of operation of an HT-ATES, the hot and cold wells are established. This means that initially, the volume of both wells is zero and the temperatures are equal to the ambient groundwater temperature. To model a full year with equal starting conditions, an initial temperature of 70°C and an initial volume of 300 000 m³ are set to the hot well. For an explanation on how these values were derived, see Appendix B. The ambient groundwater temperature is set to 12°C.

Parametrization in TESPy

To solve the energy system model in TESPy, several parameters have to be set for the components. In all connections, water is used as a fluid. Only in the heat pump circuit ammonia is set as a working fluid. For the GTD well, an extraction temperature of 76.5°C is set. The heat loss at the connected heat exchanger is 2K.

The capacity of the heat pump is limited by setting the maximum thermal output for the condenser. The exact value is design-specific and will be discussed in the results section. For the compressor, an isentropic efficiency of 0.85 is assumed. As the heat pump operates near the phase change boundaries of the working fluid, precise settings for the pressure and temperature are crucial to correctly determine the state of the fluid. Figure 7 illustrated the settings for the heat pump: the pressure at the outlet of the condenser (3) is set such that the fluid is fully condensed at a specific supply temperature that the condenser should produce for the heat sink. This condensation pressure is retrieved from the ph-diagram of the working fluid using the CoolPropsSI function. Similarly, at the evaporator side, the fluid should be in full liquid state at the temperature of the heat source. The pressure in connection (1) is adjusted accordingly to achieve this state.

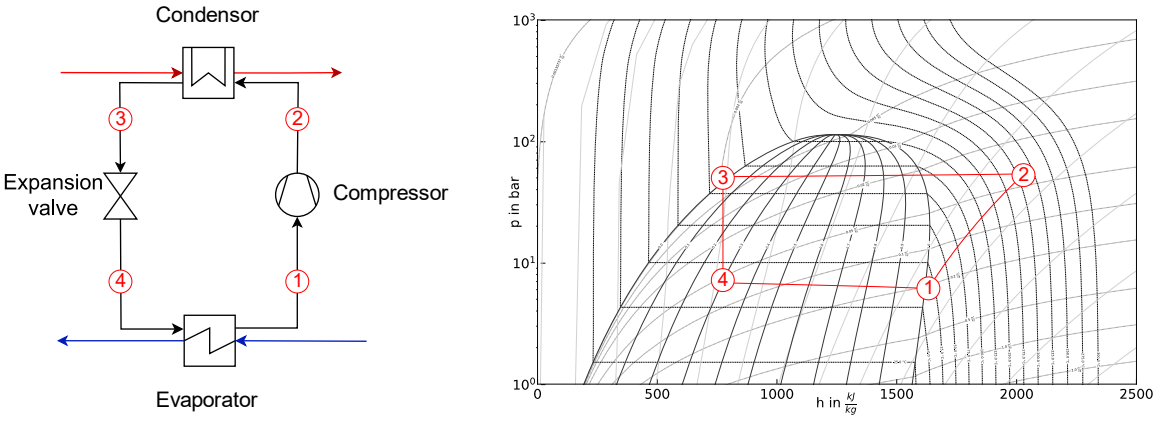

Figure 7 Heat Pump settings in TESPy corresponding to the ph-diagram of the working fluid (from author)

Furthermore, flow limitations are defined for some connections. The GTD well has a maximum flow of 400 m³/h. However, the brine in the GTD has a different density and heat capacity compared to water. Since these properties cannot be adjusted in TESPy, water is used as a working fluid and the maximum flow is set to 375 m³/h which would yield the same thermal output as 400 m³/h with the fluid of the GTD well. The flow limitation in the HT-ATES is equally set to 375 m³/h such that it could be loaded at the maximum flow rate of the GTD well.

For the GTD well additional limitations apply regarding the injection temperature back into the well. The injection temperature should not fall below 20°C or exceed 68°C and the gradient of the injection temperature should not be higher than 20°C/h. Table 1 lists all the parameters that were set in the model.

Table 1 Simulation parameter values for the energy system model and the HT-ATES

Component	Parameter	Value
HT-ATES	Initial volume hot well	300 000 m³
	Initial temperature hot well	70°C
	Groundwater temperature	12°C
	Maximum flow rate	375 m³/h
Heat pump	Fluid	NH_3
Compressor	Isentropic efficiency η_s	0.85
GTD	Extraction temperature	76.5°C
	Maximum flow rate	375 m³/h
	Minimum injection temperature	20°C
	Maximum injection temperature	68°C
	Maximum gradient injection temperature	20°C/hour
Heat Exchanger GTD	Heat loss	2K

2.3 Design Options

Three design options are simulated in this study. The first one is the reference model without a HT-ATES installed. This option allows to evaluate how much thermal energy the HT-ATES can add compared to a system without HT-ATES. Option 1 and option 2 include a HT-ATES but differ in the placement of the HT-ATES within the system.

2.3.1 Base Design

Figure 8 shows the base design in which the GTD well and the boilers (WKC) are the two heat sources in the system, and TUD and the OWD are the heat sinks. To reduce the number of connections, valves for pressure regulation are not shown. To increase the temperature coming from the GTD well (74.5°C in connection 4), the heat pump is needed. The GTD well has a maximum flow capacity of 375 m³/h. Therefore, a bypass is needed (connection 19) in case the summed flows from TUD and OWD exceed 375 m³/h. The flow direction in connection 16 can change. If the flow from the OWD network is lower than 375 m³/h, flow from the TUD is added to be able to run the GTD well at full capacity. As the thermal output for the condenser is limited, the WKC is turned on when this limit is exceeded.

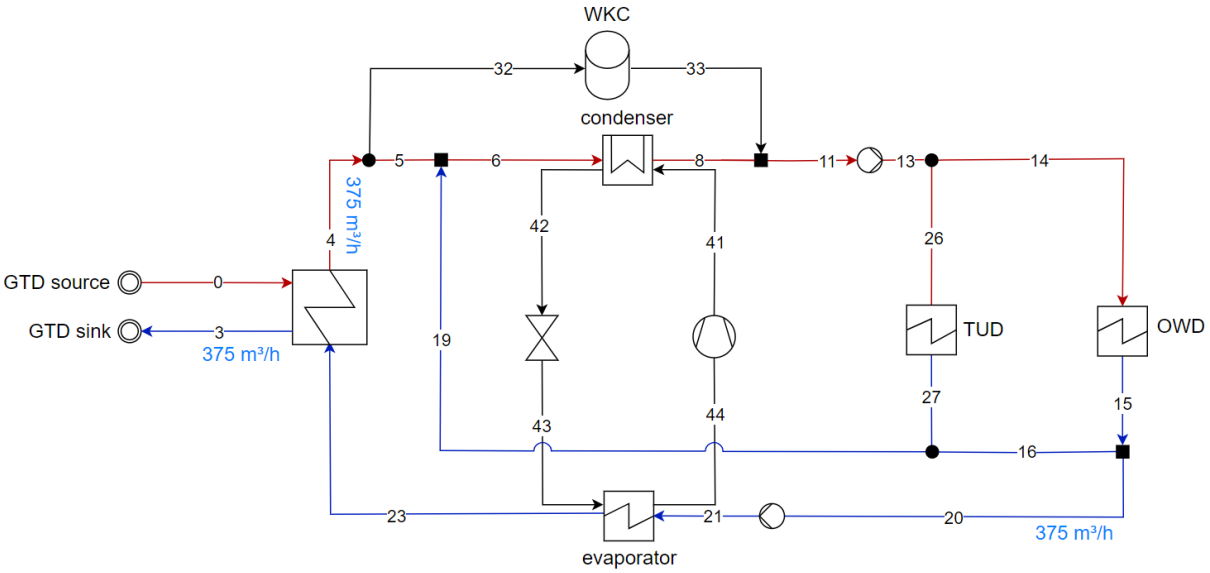

Figure 8 P&ID for the base design (from author)

2.3.2 Option 1

In option 1, the HT-ATES is added to the system. The rest of the system does not differ from the base design. The HT-ATES can either be loaded or discharged. Figure 9 shows the P&ID for both loading and discharging of the HT-ATES. Heat from the GTD well is injected into the hot well of the HT-ATES through connections 34 and 35 in loading mode. In discharging mode, the HT-ATES is connected behind the evaporator (connection 22) and thus uses the cool temperatures at the output of the evaporator to extract heat from the hot well. The flow through the evaporator is thus limited to 750 m³/h which is the sum of the maximum flows through the GTD and the HT-ATES heat exchangers. If the summed flows from TUD and OWD exceed this limit, the surplus flow is directed through the bypass (connection 19). As the hot well temperatures can reach a maximum of 74.5°C as injected from the GTD well, the flow coming from the HT-ATES (connection 29) also has to pass through the WKC or the heat pump to reach the supply temperatures needed for TUD and OWD.

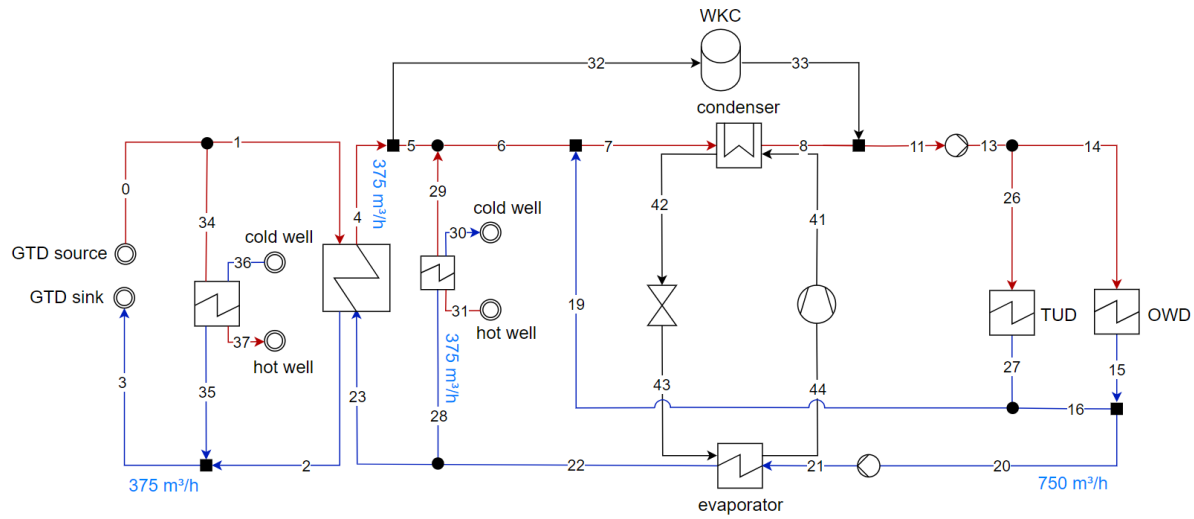

Figure 9 P&ID for design option 1 showing both charging and discharging of the HT-ATES (from author)

2.3.3 Option 2

In option 2, the charging of the HT-ATES is the same as in option 1. For the discharging mode, the HT-ATES is connected in the bypass instead of behind the evaporator (Figure 10). Therefore, the flow through the evaporator is again limited to 375 m³/h as in the base design. In case the total flow coming from OWD and TUD exceed 750 m³/h, a bypass is needed (connection 19).

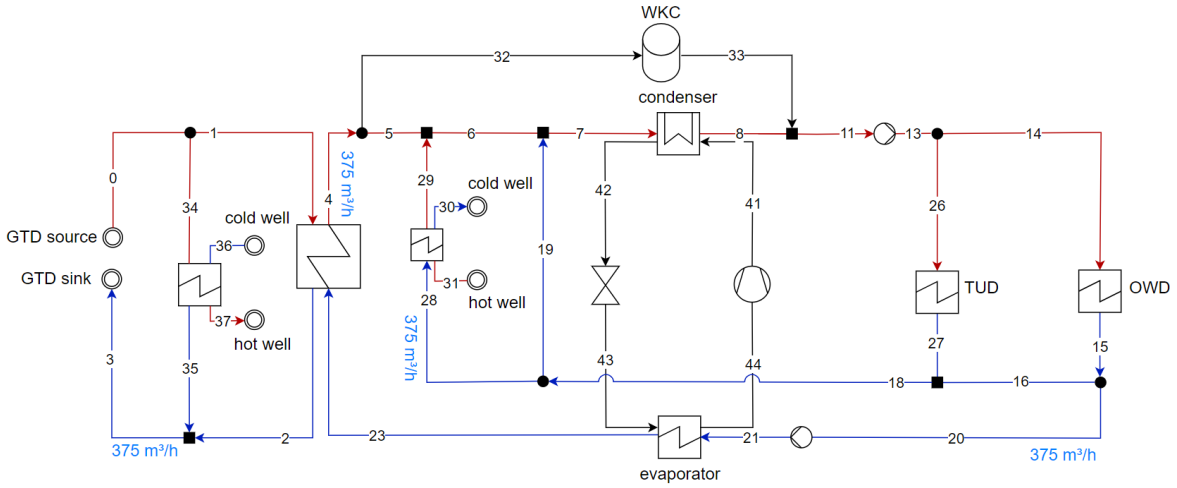

Figure 10 P&ID for design option 2 showing both charging and discharging of the HT-ATES (from author)

2.3.4 Modes of Operation in the Energy System Model

To run the model, three main modes of operation are distinguished based on the heat demands of TUD and OWD:

1. *Low heating demand:* The GTD well runs at full capacity (375 m³/h). Part of that flow is used to cover the heat demand of the consumers and the remaining flow is used to load the HT-ATES. In order to have a balanced HT-ATES, the loading is scheduled to start in August. From end of April to end of July, the GTD well runs at the flow rate that is determined by the consumers (< 375 m³/h). The heat pump is needed to reach the supply temperatures of the consumer but runs in part load. Figure 11 shows the operation of the GTD well for the two options.

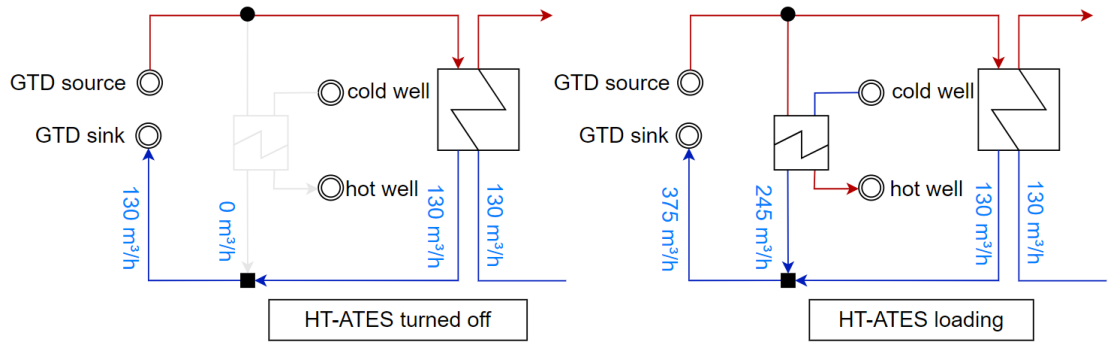

Figure 11 Two modes of operation of the GTD well for low heating demands (from author)

2. *Medium heating demand:* For medium heating demands, the summed flow of OWD and TUD is always above 375 m³/h. Therefore, the GTD well runs at full flow capacity. As long as the HT-ATES can be discharged, it supplies heat to the system.

Depending on the required heat demand and supply temperatures, the thermal output of the heat pump is defined.

3. *Peak demand:* At peak demands, the GTD well and HT-ATES are discharged as much as possible and the heat pump runs at full capacity. Additionally, the WKC is turned on to cover the heat demand of the consumers.

These modes are the same for all design options. Only in the base design, the loading and discharging of the HT-ATES is not applicable. More detailed sub-modes are defined to account for changes in flow directions. Also, different modes are required depending on whether the HT-ATES can be discharged or if it is shut down. As either TUD or OWD always needs a supply temperature above the GTD well temperature in the demand data set (see Figure 3), the heat pump is activated in all modes of operation. The model switches on an hourly basis between the modes.

In the model's code, the required mode is selected using an if-else structure. A simplified version of the decision tree for the design options with HT-ATES is shown in Figure 12. From the heat demand, supply and return temperature, the total flow in the system is computed for each hour of the year. If this flow rate is below 375 m³/h, a sub-mode within the *low heating demand* modes is chosen. It is distinguished between a sub-mode in which the HT-ATES is charged, and a sub-mode in which the HT-ATES is turned off (see also Figure 11). The period during which the HT-ATES is operated, is scheduled. The total input data set contains 8760 hours, which is a full year. Based on the hour of the year, the model decides whether to charge the HT-ATES or not. For example, if the HT-ATES is set to be off from end of April to end of July, the loading mode is chosen if the hour of the year is below 2800 (end of April) or above 5000 (end of July).

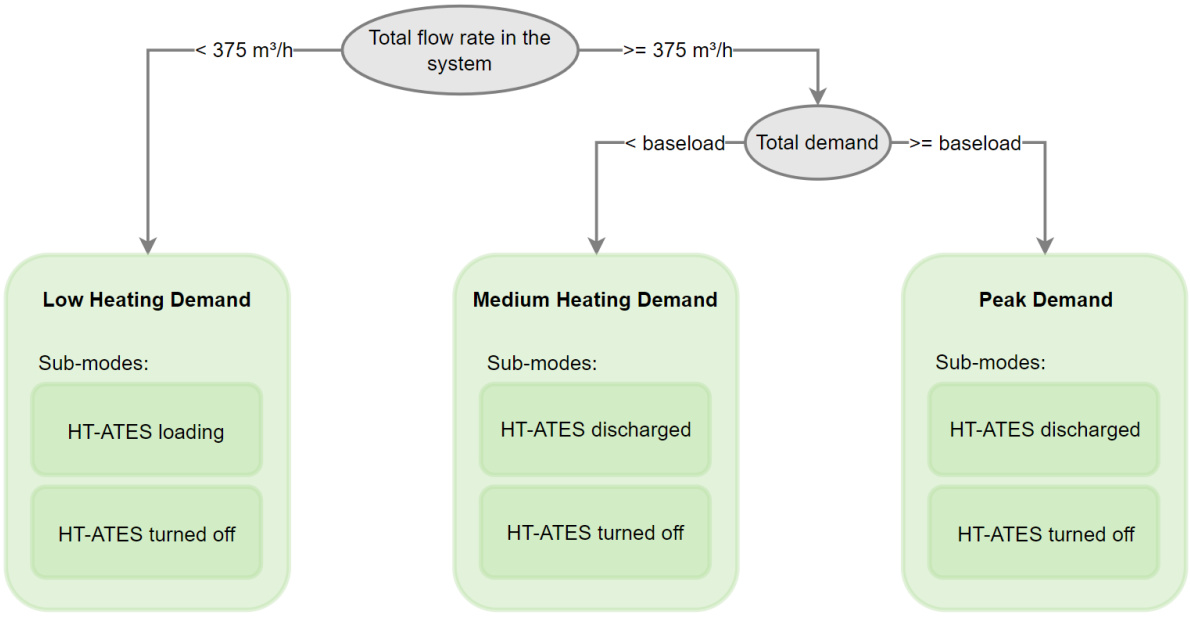

Figure 12 Schematic of the mode selection in the energy system model (from author)

If the total flow rate in the system is above 375 m³/h, an if-else statement checks whether the summed demand of OWD and TUD is above or below a specified baseload. If the demand is below baseload, the WKC in the system is not needed and a *medium heating demand* mode is chosen. Above baseload, the WKC is turned on and the model selects a *peak demand* mode. The exact value of the baseload, which is the total thermal output that can be covered

by the heat pump, the GTD well and the HT-ATES, depends on several parameters: the condenser capacity, the supply and return temperature needed in the system as well as the hot well temperature in the HT-ATES. Therefore, the value that is set for the baseload is used as a preliminary filter to choose a mode, but further checks are implemented to assure that the right mode was chosen. For example, if the demand is above baseload and the model solved a peak demand, but the WKC then consumes thermal energy instead of producing it, the mode is switched to medium demand and the WKC is turned off. This means that the model sometimes has to iterate until the correct mode is found. For a condenser capacity of 10 MW, it was found that setting the baseload to 19 MW is a good approximation.

Once the model correctly chose between medium demand and peak demand, two modes exist depending on whether the HT-ATES can be discharged or not. This depends on the hot well temperature and the value to which the cut-off temperature of the system is set. If the hot well temperature falls below the cut-off temperature, the HT-ATES is not discharged. In section 3.1, it is explained how the cut-off temperature is determined.

For the base design, the decision tree is the same as shown in Figure 12. Since the HT-ATES is not included in the base design, the sub-modes do not apply. The operational time to run a full year data set is approximately three hours for the base design. Due to the numerical HT-ATES model and the additional modes in the design options with HT-ATES, it takes approximately four and a half hours to simulate a full year for design options 1 and 2.

2.4 Sensitivity Analysis

In the previous section, the different design options and operational modes were described. These will remain unchanged throughout the study. To analyze the system's robustness, each design option is modeled for multiple scenarios. The following scenarios are modeled (for a summary, see Table 2):

Base Case

First, a 'base case' is run with the input data as presented in Figure 2 and Figure 3. The base case helps to elaborate general differences between the design options.

Adjusting the heat pump size

When dimensioning the heat pump, the aim to cover 85% of the annual heat demand with renewable energy is used as a guideline. Since the heat pump's size significantly influences acquisition costs, oversizing should be avoided. Conversely, undersizing the heat pump results in inefficient operation. In the model, the heat pump size is adjusted by defining the condenser capacity. A condenser capacity of 6 MW, 8 MW, 10 MW and 12 MW is modeled.

Reduction in supply and return temperatures

Better insulation of the buildings in future could reduce the supply and return temperatures in the network. Especially newer buildings that might be connected to the network in future, are more energy efficient and require lower supply temperatures. To explain the influence of reducing the temperatures to the performance of the system, an exemplary peak demand and medium demand situation is analyzed with adjusted temperatures. Then, the model is run for a full year with supply and return temperatures decreased by 2.5°C and 5°C separately.

Increase in heat demands

The maximum flow rate to discharge the HT-ATES is set to 375 m³/h. As this limit is not reached throughout the year, it is investigated whether increasing the demands and thereby increasing the flows in the HT-ATES can increase the heat supplied by the HT-ATES. First, an overall increase in the demands by 50% is simulated. Secondly, a scenario in which TUD demands decrease by 55% and OWD demands increase by 300% is modeled. These are the demands as predicted for the year 2042 and is referred to as 'scenario 4'.

Reducing the pump rates of the GTD well

In general, the merit order of the heat sources is set such that the GTD well is run at maximum, and any additional heat demand is covered by the HT-ATES as long as the hot well temperature is above the cut-off temperature. To reduce pumping costs of the power intensive circulation pump in the GTD well, there is an interest in lowering the pump rates. Therefore, it is investigated how prioritizing the HT-ATES in the merit order affects the total system power consumption. This means increasing the flow rate in the HT-ATES and reducing the flow rate in the GTD well. Furthermore, two loading strategies for loading the HT-ATES in summer are compared: loading the HT-ATES at a low flow rate over an extended period or loading it in a short period at maximum flow rate.

Table 2 Summary of all cases modeled in the study

Scenario/ Adjusted Parameter	**Options**	**Modeled Period**
Base Case	-	Full year
Condenser Size	• 6 MW • 8 MW • 10 MW • 12 MW	Full year
Supply Temperatures	• Reduced by 2.5°C • Reduced by 5°C	• 1 hour at peak demand • 1 hour at medium demand • Full year
Return Temperatures	• Reduced by 2.5°C • Reduced by 5°C	• 1 hour at peak demand • 1 hour at medium demand • Full year
Heat Demands	• TUD +50% and OWD +50% • TUD -50% and OWD +300%	Full year
Merit Order	• Adjust flow ratio between GTD well and HT-ATES	1 hour at peak demand
Loading Strategy of HT-ATES	• Fast loading (approx. 3 months) • Slow loading (approx. 6 months)	Full year

2.5 Performance Indicators

To evaluate the different design options and scenarios as objectively as possible, the system's performance regarding predetermined indicators is analyzed. In the following, the assessment of these PIs is explained. All necessary parameters for computing the PIs were obtained from the model's results. If the model failed to solve all 8760 data points without errors, a filter was applied to exclude unrealistic results before calculating the PIs. This filter

removed negative values for the thermal output of the compressor and WKC, as well as data points where the maximum condenser capacity was exceeded.

As stated in the introduction, the main objective of using renewable heat sources and HT-ATES systems is to reduce GHG emissions. For the project at hand, GHG emissions mainly arise from using the gas fired boilers when the heat demands are too high to be covered with only the GTD and the HT-ATES. Several boilers and a CHP are installed on campus. For simplification, all boilers and the CHP were reduced to one component, called WKC, in the model. Therefore, the share of heat supply coming from the WKC is used to assess GHG emissions in the model. This value can directly be retrieved from the energy system model.

To operate the GTD well, the HT-ATES and the heat pump, electricity is needed in several components. The electricity used in the system is considered renewable because it is generated from solar and wind energy. However, the system is more efficient if the same thermal energy can be supplied using less electricity. To assess electricity consumption, the power needed for the compressor of the heat pump and for the circulation pumps of the GTD well and the HT-ATES is considered. Other circulation pumps in the network are neglected due to their relatively low electricity consumption compared to the energy needed to deliver fluid from the subsurface. While the electricity consumption of the compressor is computed in the energy system model, the circulation pumps for operating the GTD and HT-ATES are not included in the model. Estimations on the power consumption per flow rate for these pumps were provided (A. Medema, personal communication, May 17, 2024). Based on these estimations, characteristic curves for the pumps can be computed as displayed in Figure 13. As can be seen, the GTD well pump consumes far more electricity than the HT-ATES pump mainly because the GTD extracts heat from a much deeper level.

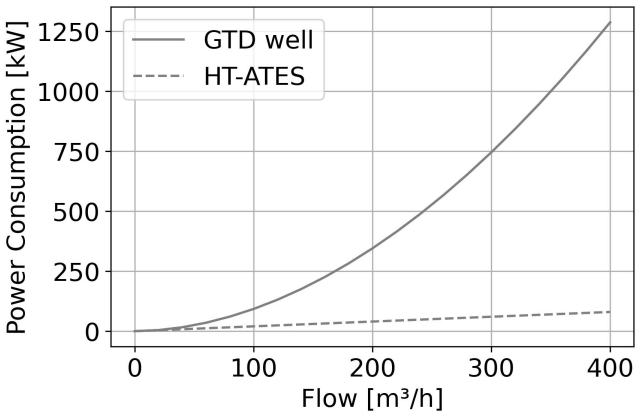

Figure 13 Estimated power consumption for circulation pumps (A. Medema, personal communication, May 17, 2024)

The COP of a heat pump describes the thermal output produced per unit of electrical energy that is consumed and is a common PI used for heat pumps. At maximum theoretical efficiency, a heat pump resembles a Carnot cycle and the maximum COP is therefore:

$$COP_{max} = \frac{T_H}{T_H - T_C} \tag{5}$$

where T_H is the temperature of the hot reservoir in K and T_C the temperature of the cold reservoir in K. Therefore, the COP highly depends on the supply and return temperatures in the system and represents only the momentary efficiency of the heat pump. In this study, the

seasonal COP (SCOP) is assessed, considering variations in the heat pump efficiency over one year. The $SCOP_{HP}$ is computed as follows:

$$SCOP_{HP} = \frac{Q_{condenser,total}}{W_{compressor,total}} \quad (6)$$

where Q is the total thermal energy produced by the condenser in one year in MWh and W the electrical energy consumption of the compressor over one year in MWh. Both values are retrieved from the energy system model. TESPy computes these values depending on the working fluid used in the heat pump and the required pressure and temperature levels at the inlets and outlets of the condenser and compressor respectively.

Besides the SCOP of the heat pump, the SCOP of the total system is also considered. It is defined here as the total thermal energy produced from renewable sourced in the system divided by the total electricity consumption of the system over one year:

$$SCOP_{System} = \frac{Q_{system,total}}{W_{system,total}} \quad (7)$$

The thermal energy $Q_{system,total}$ includes the thermal energy supplied to the system by the GTD well and the HT-ATES. The thermal energy that is needed from the GTD well to load the HT-ATES is not counted in. The electrical energy $W_{system,total}$ is the energy consumed by the compressor and the circulation pump of the GTD well. The circulation pump in the HT-ATES is neglected here due to its comparably low electricity consumption (see section 3.2.5).

The efficiency of the HT-ATES system is assessed with the thermal recovery efficiency η_{th}. It describes the ratio between the extracted thermal energy E_{out} and the injected thermal energy E_{in} over a defined time period (Bloemendal & Hartog, 2018):

$$\eta_{th} = \frac{E_{out}}{E_{in}} \quad (8)$$

For the extracted and injected thermal energy, the values for the thermal output of the heat exchanger that is connected to the HT-ATES is derived from the energy system model.

Table 3 summarizes the main indicators used in this study. These PIs can all directly be evaluated using the model's results. Besides, more aspects that are relevant when evaluating HT-ATES and geothermal system are briefly considered in the discussion section. The design options will be compared in terms of their financial performance, including both expenses and revenues of the system. The effect of the HT-ATES on the subsurface is evaluated by comparing the volume and the temperature difference between the HT-ATES and the surrounding groundwater. Additionally, the sustainability of the GTD well is assessed by considering its operational lifetime.

Table 3 Assessment of Performance Indicators

Performance Indicator	Assessment Parameter
GHG emissions	Thermal energy supply from WKC
Electricity consumption	• Energy consumption of the compressor • Energy consumption of circulation pumps in GTD well and HT-ATES
SCOP heat pump	Generated thermal energy of the condenser / consumed electrical energy by the compressor over one year
SCOP system	Generated thermal energy in the system / consumed electrical energy in the system over one year
Thermal recovery efficiency of HT-ATES	Extracted thermal energy / injected thermal energy

3 Results

In the following chapter, the different design options are first compared in general using the unchanged input data (base case). In the sensitivity analysis, the results of the model for different sizes of the condenser are presented to dimension the heat pump. Then, the supply and return temperatures as well as the demands in the input data are adjusted. Furthermore, adjustments to the pump rate of the GTD well are analyzed. An evaluation of the PIs is provided at the end of each subsection.

3.1 Comparison of the Design Options

To demonstrate the key differences between the design options, the base case is run. Here, the condenser is limited to a capacity of 8 MW. As will be explained in section 3.2.1, a condenser size of 8 MW is required to supply 85% of the annual heat demand with renewable energy. Figure 14 shows the proportions of the different heat sources in the total demand over one full year. The thermal energy used from the GTD well to load the HT-ATES is shown with negative sign. In all options, the WKC is needed only during peak demands in winter. During low demands in summer, the GTD can fully cover the demands. However, the heat pump is still needed to increase the temperatures coming from the GTD to the required supply temperature. Moreover, the heat pump decreases the injection temperature into the GTD well and therefore allows for more energy extraction from the GTD. Thus, the compressor still covers a small proportion of the heat demand in summer.

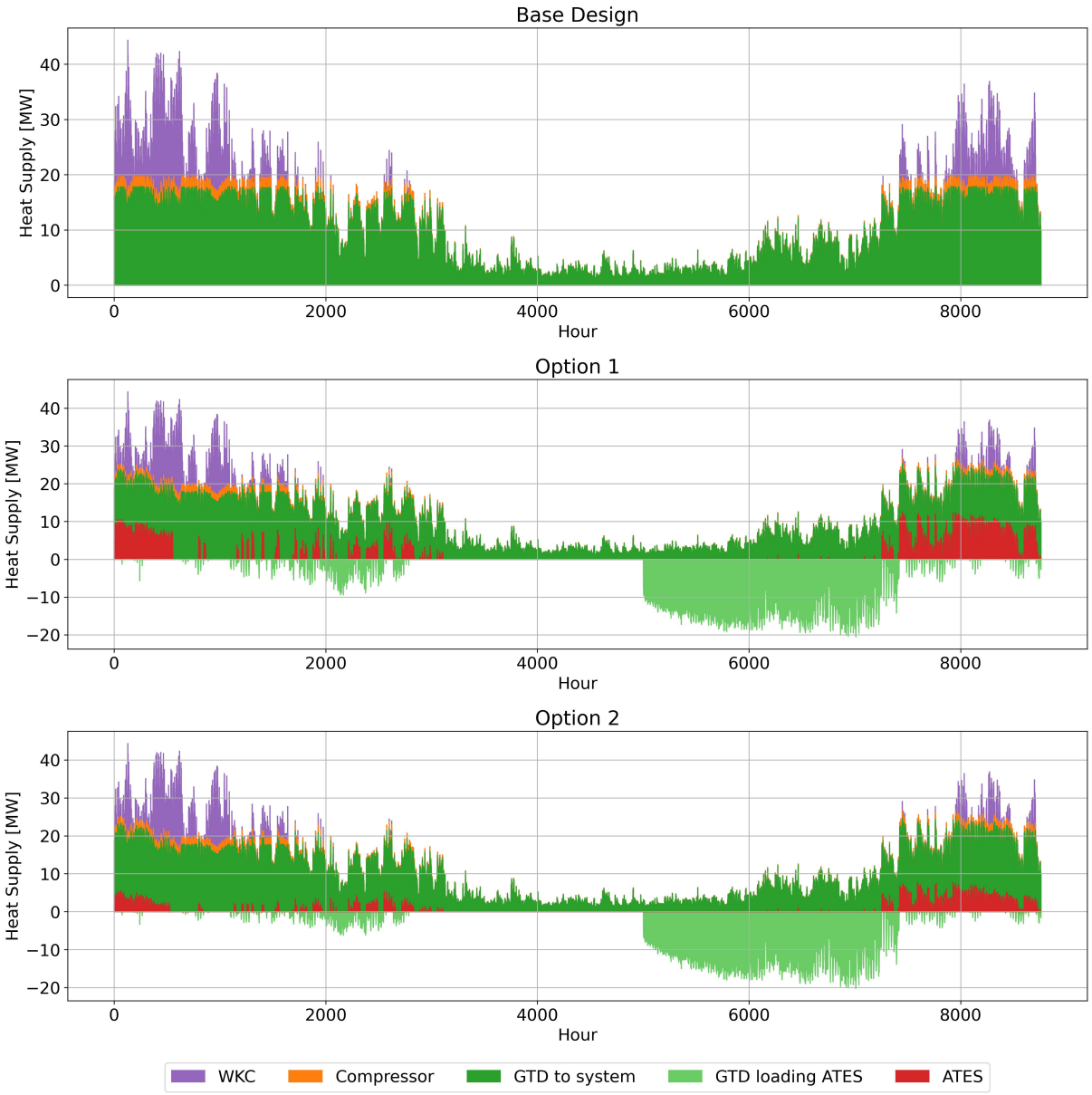

Figure 14 Comparison of heat supply per heat source for all design options over one year

In option 1 and 2, the HT-ATES is loaded during three months in summer and the discharging starts in November, at approximately hour 7000 in Figure 14. The HT-ATES stops supplying heat when the temperature in the hot well is too low to add energy to the system. This is seen as a clear cut in the plots in January (around hour 500). During spring, the HT-ATES is switching between charging and discharging mode which can be observed as an irregular share of the heat supply in the figure above.

Compared to the base design, option 1 adds thermal energy from the HT-ATES to the system but also reduces the thermal energy supply from the GTD well to the system. This is because the maximum flow through the evaporator in the base design is 375 m³/h whereas in option 1, 750 m³/h can go through the evaporator. Depending on the capacity of the condenser and the COP of the heat pump, the evaporator extracts a certain amount of thermal energy from the system and thus reduces the return temperature from the consumers to a lower level (connections 21 and 22 in Figure 9). According to the heat transfer equation, a higher flow rate results in a smaller temperature difference for a given

amount of heat transfer. Consequently, the temperatures in connection 22 in option 1 are generally higher than the temperatures in the same connection in the base design. Since this temperature in turn defines the temperature difference at the heat exchanger connected to the GTD, the thermal energy transferred from the GTD is about 10% less in option 1 compared to the base design.

The design of option 2 ensures that the flow through the evaporator is kept the same as in the base design (375 m³/h). Consequently, compared to the base design, the HT-ATES primarily adds heat energy to the energy that could already be extracted from the GTD if there were no HT-ATES. On the other hand, the temperatures going into the heat exchanger to discharge the HT-ATES are higher in option 2 than in option 1 (connection 28 in Figure 9 and Figure 10). In option 1, the flow used to discharge the HT-ATES is cooled down by the evaporator while in option 2 the temperatures in connection 28 correspond to the return temperatures of OWD and TUD. Consequently, the HT-ATES can supply more heat in option 1 than in option 2. These principal differences are shown in the simulation throughout the year. In Figure 14, the share of the thermal energy supplied to the system by the GTD well is the same in the base design as well as in option 2. In option 1, the GTD supplies less thermal energy to the system. The share of the HT-ATES in turn, is higher in option 1 than in option 2. The total thermal energy supplied by the GTD well including the energy needed to load the HT-ATES is more in the options with HT-ATES than in the base design.

In Figure 15 the summed energy per heat source over one year is shown. The thermal energy used from the GTD well to load the HT-ATES is again shown with negative sign. For better comparison, Table 4 shows the absolute values. Adding the HT-ATES to the system in options 1 and 2 reduces the proportion of the WKC and the compressor compared to the base design by 31% and 29% respectively. In both option 1 and 2, the temperature going into the condenser is increased (connection 7 in the P&ID). Thus, the condenser and consequently the compressor supply less energy compared to the base design. When the heat pump runs at full capacity, more flow is allowed through connection 7 in the options with the HT-ATES, because the temperature difference between connections 7 and 8 is smaller than in the base design. This again reduces the energy that has to be supplied by the WKC.

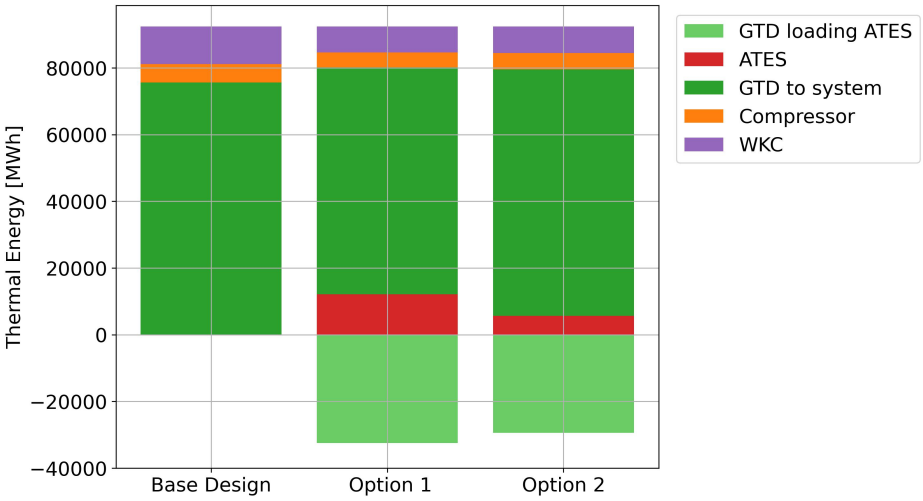

Figure 15 Annual thermal energy per heat source for all design options

Table 4 Annual thermal energy in MWh per heat source for all design options as shown in Figure 15

	Base Design	Option 1	Option 2
ATES	0	12 044	5 681
GTD total	75 676	100 214	103 359
GTD to system	75 676	67 731	73 900
GTD loading ATES	0	32 483	29 459
Compressor	5 475	4 452	4 910
WKC	11 270	7 769	7 965
Total	92 421	124 480	121 915

Moreover, it becomes apparent that the compressor has a slightly higher output in option 2 than in option 1 even though the capacity of the condenser is limited to 8 MW in all options. This can be explained again with the higher flows going through the evaporator in option 1. If more flow is needed in connection 21 (see Figure 9), the returning flow from TUD (connection 27) is added to the returning flow from OWD (connection 15). Especially for higher demands, TUD has a higher return temperature than OWD. This means that in option 1, higher temperatures are going into the evaporator in connection 21 than in option 2. As this temperature defines the COP of the heat pump, option 1 has a slightly better COP than option 2. A better COP means that for the same thermal output, less energy is provided by the compressor and more by the evaporator. Considering a full year, option 1 has a $SCOP_{HP}$ of 5.34 compared to a $SCOP_{HP}$ of 4.88 in option 2. The base design has a $SCOP_{HP}$ of 4.81.

Option 1 and option 2 also differ regarding the temperature changes in the cold well. Figure 16 shows how the volume and the temperatures in the HT-ATES change over one year. As the flow into the HT-ATES and the injection temperature from the GTD is the same for option 1 and option 2, the volume of both wells and the temperature of the hot well is the same in both options. The volume is computed by cumulating the flows into the cold and hot well respectively. The initial volume of the hot well is set to 300 000 m³ and the initial temperature to 70°C as explained in Appendix B. The volumes and temperatures at the beginning and the end of the year do not match. Currently, more flow is injected than extracted resulting in an unbalanced system. However, under real operation conditions, the volume and temperature in the hot well will vary, too.

The injection temperature into the cold well is lower in option 1 as the HT-ATES is connected after the evaporator. Consequently, the cold well temperature does not exceed 48°C. The injection temperature in option 2 is defined by the return temperatures of TUD and OWD, reaching up to 60°C. These different cold well temperatures result in different thermal recovery efficiencies of the HT-ATES. Option 1 has a thermal recovery efficiency of 0.37 and for option 2 it is 0.19 (see Figure 49 in Appendix C). The lowest temperature in the cold well depends on the ambient groundwater temperature which is set to 12°C in the model. This temperature is reached during the loading of the HT-ATES when the cold well is empty resulting in a theoretically negative volume.

The different cold well temperatures also explain the difference in the thermal energy loaded from the GTD well into the HT-ATES during loading periods. In option 1, about 32 500 MWh are loaded into the HT-ATES which is approximately 3 000 MWh more than in option 2. The thermal energy from the GTD well is extracted by directing flow from the cold well through

the heat exchanger connected to the GTD well. The lower the cold well temperature, the more thermal energy can be extracted at the heat exchanger.

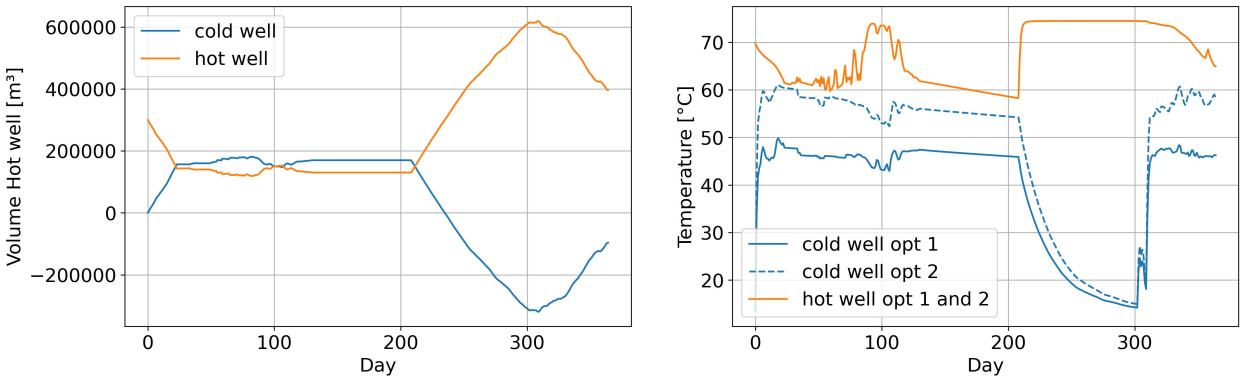

Figure 16 Volume and temperature changes in the HT-ATES

The cut-off temperature of a HT-ATES describes the lowest temperature at which the HT-ATES can be run to add energy to the system (Drijver et al., 2019). In the model, the cut-off temperature for the HT-ATES is set to 61°C. If the temperature in the hot well falls below this temperature, the HT-ATES is shut down and then the P&ID of options 1 and 2 are the same as in the base design. 61°C is the return temperature of TUD during cold outside air temperatures and the governing temperature in the bypass in the base design (connection 19). Only when the OWD flow exceeds 375 m³/h, the temperature in the bypass is a mixing temperature of the return temperature of OWD and TUD. In option 1, the HT-ATES might add thermal energy to the system as long as the temperatures of the hot well are higher than the temperatures at the outlet of the evaporator (connections 22 and 28), but if the temperatures in the bypass are higher than in the HT-ATES, it is more efficient to direct the flow through the bypass instead of the evaporator and the HT-ATES. In other words, if the returning flow of TUD at a temperature level of 61°C is cooled down in the evaporator and then heated up to a temperature below 61°C through the HT-ATES, thermal energy is lost in the system. Therefore, if the hot well temperature falls below the cut-off temperature, the base design is the most efficient design. This is possible because the thermal energy that the evaporator draws from the system is the same in all options but with different flows and temperature differences.

In Figure 17, the temperatures injected back into the GTD are shown for the base design and option 1. These temperatures are 2°C warmer than the temperatures at the outlet of the evaporator due to heat losses at the GTD heat exchanger. In option 1, the injected temperatures are higher than in the base design, as long as the HT-ATES is operated. When the hot well temperature reaches the cut-off temperature, the HT-ATES is turned off and option 1 corresponds to the base design. This is highlighted with the blue areas in the figure. In this case, the flow in the evaporator is again limited to 375 m³/h. Therefore, the temperature at the outlet of the evaporator drops significantly in January when the HT-ATES is shut down. This temperature drop is also seen in the temperatures injected into the GTD well. One restriction to this configuration is the lower temperature limit of the injection temperature back into the GTD well as well as the maximum gradient in the injection temperature (see Table 1). As shown in the figure, the lower limit of 20°C is not reached. The upper limit of 68°C is not reached, either. The highest temperature difference between two consecutive hours is 19.2°C and therefore just within the limit of 20°C/h.

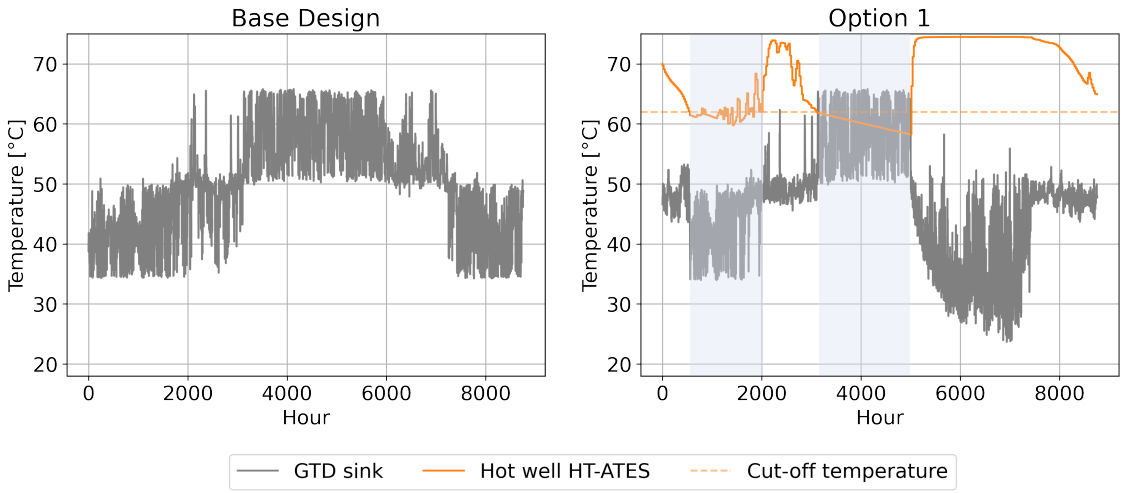

Figure 17 Comparison of GTD injection temperatures over one year (blue areas: HT-ATES is shut down)

Table 5 provides a summary of the PIs as introduced in the methodology section for the base design and the two design options with HT-ATES. The evaluation is based on the results of the base case as presented in Figure 14 and Figure 15.

If the GHG emissions are directly linked to the thermal energy supplied by the WKC, a reduction of 31% and 29% can be achieved in option 1 and option 2, respectively. The electricity consumption of the compressor is the lowest in option 1 as it has the best $SCOP_{HP}$ of 5.34. Compared to the base design, option 2 also has a better $SCOP_{HP}$ and a lower electricity consumption for the compressor because the HT-ATES increases the temperature at the inlet of the condenser. On the other side, the electricity consumption of the GTD well is higher in the options with HT-ATES as the loading of the hot well increases the flow rates in the GTD well compared to the base design. The GTD well pump electricity consumption is the same in option 1 and option 2, as the flow rates directed through the GTD well are the same. The difference in the thermal output of the GTD is only due to the temperature differences between the two options.

In total, the electricity consumption is higher in options 1 and 2 than in the base design. This also explains why the base design has the best system SCOP. In the system SCOP, only the thermal energy from the GTD well that is supplied to the system and the thermal output of the HT-ATES is considered in the numerator. In the denominator, the GTD well pump electricity consumption increases significantly in options 1 and 2 to load the HT-ATES. Option 2 has a lower system SCOP than option 1 due to the smaller proportion of thermal output from the HT-ATES. Finally, option 1 has a better thermal recovery efficiency for the HT-ATES than option 2 because of the lower temperatures used to discharge the HT-ATES.

Table 5 Comparison of Performance Indicators for all design options based on the base case results

Performance Indicator	Base Design	Option 1	Option 2
Annual GHG emissions			
• Q WKC [MWh]	11 270	7 769	7 965
Annual Electricity consumption			
• W Compressor [MWh]	5 475	4 452	4 910
• W GTD well pump [MWh]	5 445	8 001	8 030
SCOP Heat pump [-]	4.81	5.34	4.88
SCOP System [-]	6.93	6.41	6.15
η_{th} HT-ATES [-]	-	0.37	0.19

3.2 Sensitivity Analysis

3.2.1 Dimensioning the Heat Pump

The dimension of the heat pump in the model is defined by the capacity of thermal energy that the condenser can supply. Based on a general cost-benefit estimation, the aim is to meet 85% of the total annual demand using sustainable heat sources. As the size of the heat pump influences the thermal energy that can be supplied by the GTD well and the HT-ATES, the system as a whole must be considered to dimension the heat pump.

The capacity of the condenser together with the supply and return temperatures in the system determine the thermal energy that is drawn from the system at the evaporator. This in turn defines the temperature going into the heat exchanger at the GTD well and therefore the thermal output of the GTD well. The bigger the condenser capacity, the colder the temperatures at the outlet of the evaporator and the more thermal energy is supplied by the GTD. In option 1, this dependency is also true for the HT-ATES while in option 2, the thermal output of the HT-ATES does not depend on the outlet temperature of the evaporator. This is shown in Figure 18. In option 1, the proportion of thermal energy supplied by the HT-ATES increases with the size of the condenser while in option 2, the HT-ATES supply remains constant. Assuming that the compressor is powered by renewable wind and solar energy, a capacity of 8 MW for the condenser is sufficient to reach the 85% goal in all three design options. With the HT-ATES installed, even the 6 MW condenser seems sufficient in the simulation. However, the real capacity of the heat pump depends on the actual heat pump model and its components such as the working fluid or the area of the heat exchangers for the evaporator and the condenser.

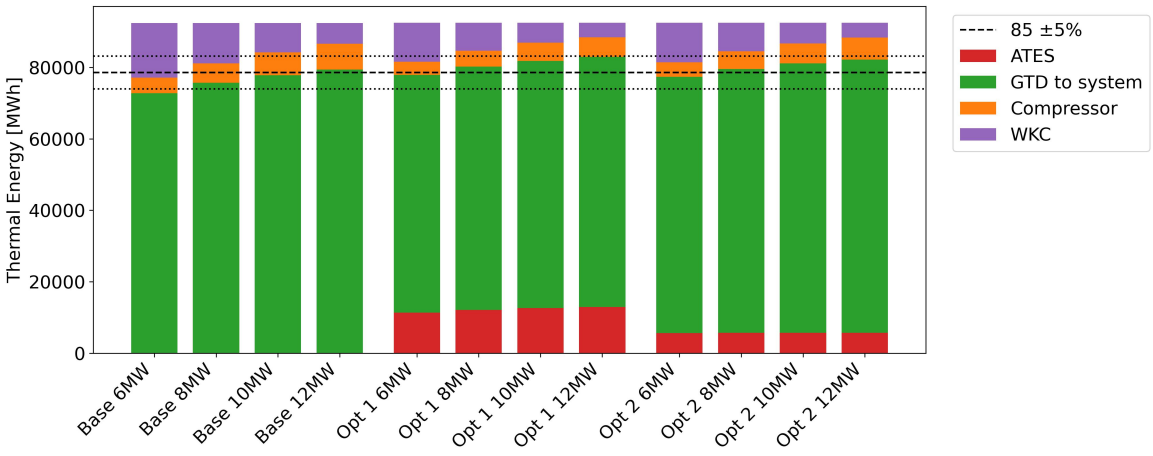

Figure 18 Annual thermal energy per heat source depending on condenser size

The volume of the HT-ATES is the result of the accumulated flows that are injected and extracted. These flows are computed by the energy system model and depend only on the demands and temperatures required by the consumers. Therefore, the volume of the HT-ATES does not change with the size of the condenser. The same applies to the hot well temperature. It is defined by the extraction temperature from the GTD well and cools down depending on the flows extracted from the hot well. Only in option 1, the cold well temperatures are influenced by the size of the condenser (see Figure 19). The cold well temperature slightly decreases with an increase in the condenser capacity. Similarly, an increased condenser size also decreases the temperature that is injected back into the GTD well. For all tested condenser sizes, the injections temperatures are within the limitations of 20°C to 68°C.

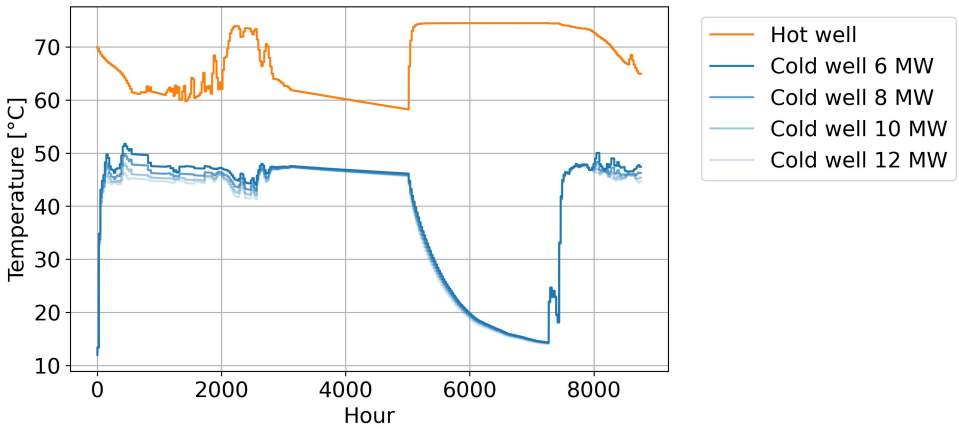

Figure 19 Temperature changes in the cold and hot wells in design option 1 depending on condenser size

In Table 6, the PIs for design option 1 depending on the condenser size are summarized. The assessment of the PIs for the base design and design option 2 is shown in Table 12 and Table 13 in Appendix C. All PIs show a linear trend. In line with the thermal output of the WKC, the GHG emissions can be reduced by increasing the size of the heat pump. The annual electricity consumption grows due to an increased power consumption of the compressor. Except for minor inaccuracies in the model results, the electricity consumption of the GTD well pump is the same for all condenser sizes, as the flow rates directed through the GTD well do not change.

The smaller the condenser size, the better the SCOP of the heat pump as well as the SCOP of the system. In an ideal Carnot cycle, only supply and return temperature are relevant to compute the efficiency. Thus, the SCOP values should not change with the condenser size. In the TESPY model, however, the COP of the heat pump varies with the flow rate directed through the evaporator and the condenser. The effectiveness of transferring thermal energy at these two components depends on the ratio of the flow rates and heat capacity of the fluids on both sides of the heat exchanger (system flow and refrigerant). Also, the flow rates through the evaporator and the condenser are not the same during peak demands when part of the flow is directed through the WKC. The results in Table 6 show that in the model, even though the thermal energy extracted from the GTD well and the HT-ATES increase, the electricity consumption for the compressor increases at a higher rate. Nevertheless, the change in the SCOP values is relatively small.

The thermal recovery efficiency of the HT-ATES slightly improves with a bigger condenser size, because the thermal output retrieved from the HT-ATES increases, while the thermal energy loaded into the HT-ATES stays the same. The financial aspect of increasing the heat pump size is not represented here. However, the size of the condenser is a major factor driving the acquisition costs of a heat pump.

Table 6 Performance indicators for design option 1 depending on condenser size

Performance Indicator	**Condenser size**			
	6 MW	**8 MW**	**10 MW**	**12 MW**
Annual GHG emissions • Q WKC [MWh]	10 843	7 769	5 565	3 995
Annual Electricity consumption • W Compressor [MWh] • W GTD well pump [MWh]	 3 742 8 016	 4 452 8 001	 5 060 8 024	 5 513 8 027
SCOP Heat pump [-]	5.56	5.34	5.17	5.03
SCOP System [-]	6.60	6.41	6.25	6.12
η_{th} HT-ATES [-]	0.35	0.37	0.39	0.39

3.2.2 Reducing Supply Temperatures

Reducing the supply temperatures has a different effect on the system during peak demands than during medium demands. Therefore, peak and medium demands are analyzed separately in the following.

As can be seen in Figure 20, the supply temperature does not affect the overall performance of the system significantly in peak demand situations. The main achievement is an improvement of the COP of the heat pump. Reducing the supply temperatures decreases the temperature difference between supply and return temperature (see equation (5)). Because of the better COP, the share of the compressor is lower. This means that more thermal heat is extracted from the system at the evaporator. Consequently, the temperatures at the output of the evaporator decrease and more energy can be extracted from the GTD well in all options. In option 1, the share of the HT-ATES heat supply also increases slightly with reduced supply temperatures as the HT-ATES is connected behind the evaporator. In option 2, the share of the HT-ATES is not affected by the supply temperature.

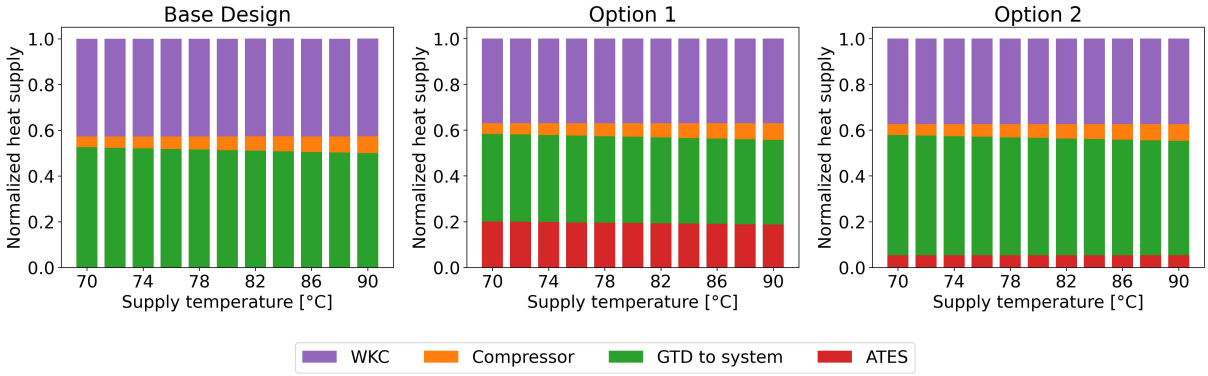

Figure 20 Influence of supply temperature on distribution of energy delivery during one hour at peak demand

During the peak demand situation shown above, the total flow in the system exceeds 750 m³/h for any supply temperature. Therefore, the flows through the HT-ATES and the GTD well are at maximum flow rate (375 m³/h) for all supply temperatures. The total flow in the system increases when the supply temperatures are reduced but the demands and return temperatures are not changed. For peak demands, this only increases the flow in the bypass. For a medium demand situation, the GTD well runs at full capacity and the flow rates through the HT-ATES increase with lower supply temperatures (see Figure 21). Under medium demand conditions, the heat pump operates in part load. With a higher flow rate in the HT-ATES, the temperatures going into the condenser are increased (connection 7 in option 1 and 2). Together with the lower supply temperatures required at the outlet of the condenser, this leads to a decrease in the thermal output from the condenser. The evaporator thus also extracts less heat energy from the system and the temperatures at the outlet of the evaporator increase for lower supply temperatures. In the figure below, this is seen in a decrease of the proportion of the GTD well for lower supply temperatures in option 1 and option 2. In option 1 this decline in enhanced due to higher flow rates in the evaporator.

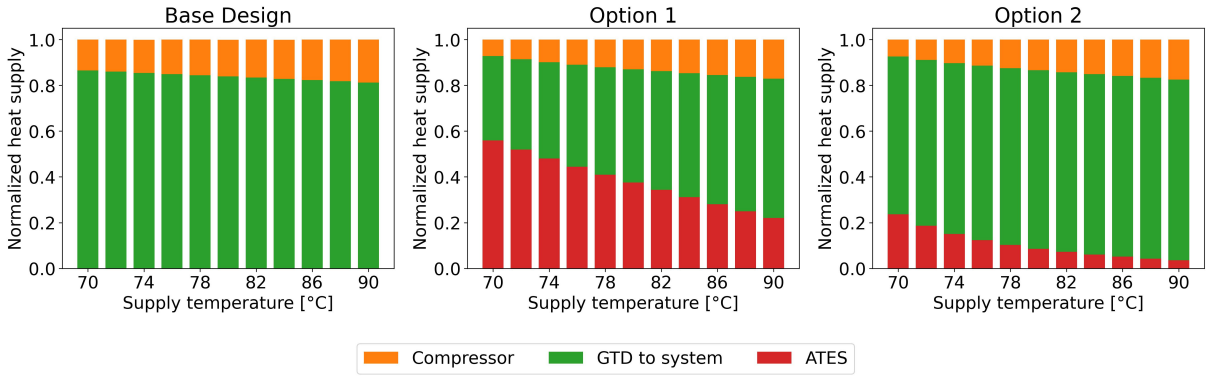

Figure 21 Influence of supply temperature on distribution of energy delivery during one hour at medium demand

Overall, the effect of reducing the supply temperature is relatively small. During peak demands, when the condenser runs at full capacity, the COP of the heat pump is improved equally in all options, but the proportion of thermal energy supplied by the WKC does not change. For medium demand situations, the proportion of thermal energy supplied by the HT-ATES increases significantly but the heat supply from the GTD well decreases at the same time. The reduction of the power consumption of the compressor is more pronounced in the options with HT-ATES than in the base design because the HT-ATES increases the temperatures going into the condenser.

Also, when looking at the results for the full year simulation, the impact of reducing the supply temperatures is very small (see Figure 22). In all options, the share of the compressor is reduced due to an improvement of the COP. Moreover, the heat pump can even be turned off when the supply temperature falls below the temperature level of the mixed flows directed through the GTD well, HT-ATES and the bypass. In the base design this leads to an increase in the heat supply from the GTD well and to a reduction of the thermal output from the WKC. In options 1 and 2, the GTD well also supplies more thermal energy. However, the proportion of the HT-ATES decreases and therefore, the share of the WKC slightly increases when reducing the supply temperature. Even though the increased flows in the system allow for more heat extraction from the HT-ATES, also less flow is available to load the HT-ATES. The temperature of the hot well decreases faster than for the regular supply temperature due to a smaller volume of the HT-ATES and the higher flows used for extraction. This is shown in Figure 23. Still, the design options with HT-ATES always require less thermal energy supply from the WKC than the base design.

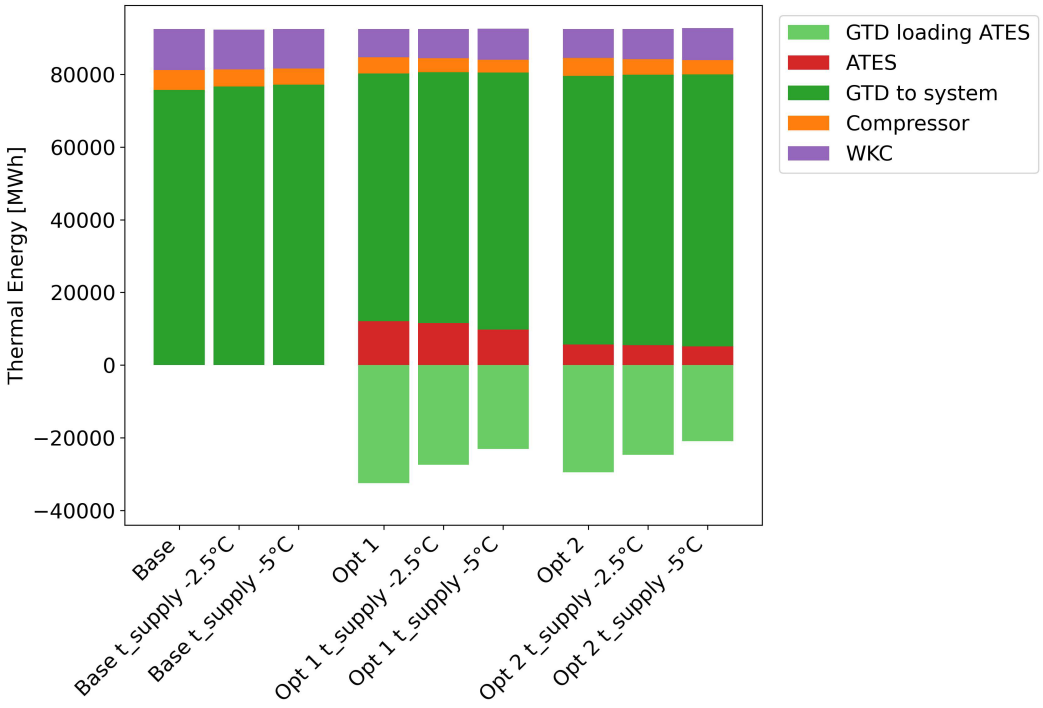

Figure 22 Annual thermal energy per heat source for reduced supply temperatures

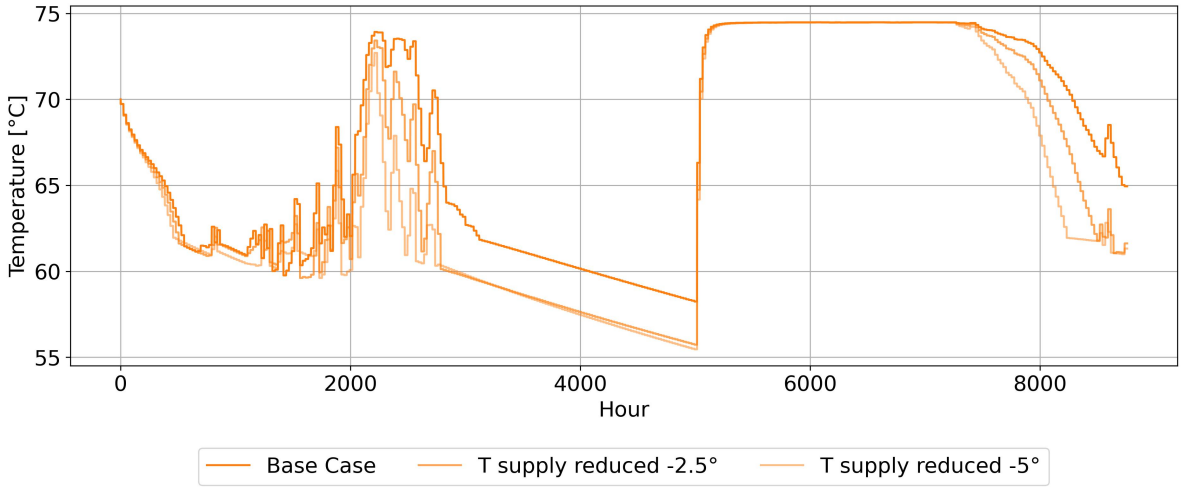

Figure 23 Hot well temperatures over one year for reduced supply temperatures

Table 7 shows how reducing the supply temperature affects the PIs for design option 1. The PIs for the base design and design option 2 are provided in Table 14 and Table 15 in Appendix C. As explained above, the GHG emissions slightly increase in design option 1 because of the reduced thermal output of the HT-ATES. Reducing the supply temperature improves the SCOP of the heat pump and therefore the annual electricity consumption of the compressor is reduced. As explained before, the electricity consumption of the compressor also depends on the flow rates directed through the heat pump. This can explain why there is no linear trend in the SCOP of both the heat pump and the system.

The electricity consumption of the GTD well pump slightly increases because of the higher flows in the system. The system SCOP improves as the sum of the thermal output of GTD well and HT-ATES increases while the annual electricity consumption of the compressor decreases. Less thermal energy can be extracted from the HT-ATES. However, also less thermal energy is injected into the HT-ATES due to the lower flow rates in the system. Overall, this leads to an improvement in the HT-ATES recovery efficiency for reduced supply temperatures.

Table 7 Performance indicators for design option 1 for reduced supply temperatures

Performance Indicator	**Reduction of Supply Temperature**		
	Base Case	**- 2.5°C**	**- 5°C**
Annual GHG emissions • Q WKC [MWh]	7 769	8 065	8 438
Annual Electricity consumption • W Compressor [MWh] • W GTD well pump [MWh]	 4 452 8 001	 3 831 8 160	 3 460 7 954
SCOP Heat pump [-]	5.33	5.40	5.34
SCOP System [-]	6.41	6.70	6.68
η_{th} HT-ATES [-]	0.37	0.42	0.40

3.2.3 Reducing Return Temperatures

The effect of reducing the return temperatures, is again considered separately for peak and medium demands. Figure 24 shows how reducing the return temperatures affects the distribution of the individual heat sources in meeting the total demand during peak demands. To standardize the results, the reduced return temperatures were assigned to both TUD and OWD. The lower the return temperature, the less thermal energy has to be supplied by the WKC because the share of heat supplied by the GTD increases in all options due to lower temperatures entering and leaving the evaporator. In option 1 and option 2, the share of heat supplied by the HT-ATES also increases with lower supply temperatures. Therefore, the gradient with which the proportion of the WKC increases is steeper in the options with HT-ATES. Reducing the return temperatures also decreases the COP of the heat pump because the temperature difference between supply and return temperature increases. During peak demands, the condenser runs at full capacity, but the share of the compressor slightly increases for lower return temperatures. However, the increase in the thermal output from the GTD well and HT-ATES is the more decisive factor when aiming for a reduction of GHG emissions.

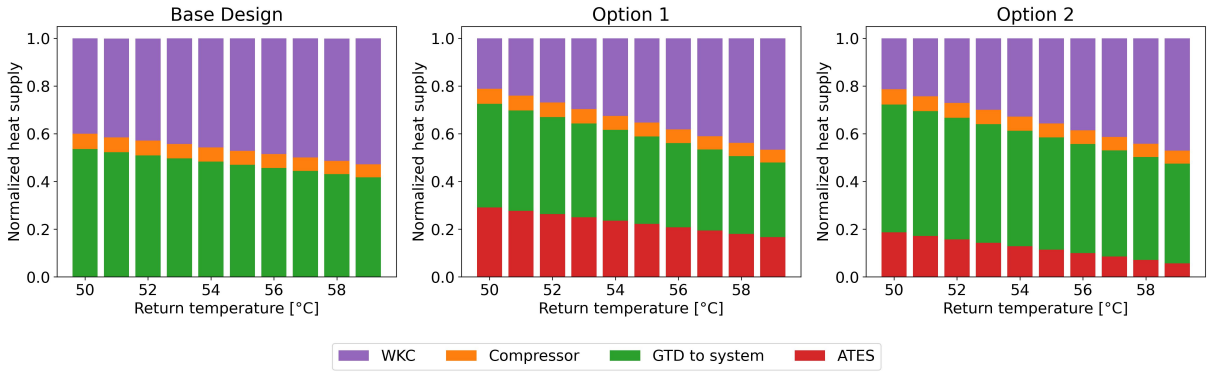

Figure 24 Influence of return temperature on distribution of energy delivery during one hour at peak demand

For medium demands, the dynamics are different (see Figure 25). Reducing the return temperatures also leads to lower flows in the system if the demands and supply temperatures are not adjusted. The total flow in the system in the peak demand situation shown above exceeds 750 m³/h and all additional flow is directed through the bypass. During medium demands, the flow in the HT-ATES decreases for lower return temperatures and the bypass is not needed. The flow through the GTD well is still constant at 375 m³/h. Therefore, in the base design, lower return temperatures lead to a higher thermal output from the GTD well. The COP of the heat pump increases with higher return temperatures but because the heat pump runs in part load, the total thermal output of the condenser and consequently the power of the compressor is increasing due to higher flows in the system. The proportion of the compressor is still lower in the options with the HT-ATES compared to the base design because the HT-ATES increases the temperatures at the inlet of the condenser (connection 7 in options 1 and 2).

In option 1, reducing the return temperatures mainly leads to an increase in the supply from the GTD well and a decrease in the supply from the HT-ATES due to lower flows in the system. In option 2, the dynamics are not linear anymore. The temperatures going into the evaporator (connection 21) increase with higher return temperatures. However, as the thermal energy extracted at the evaporator increases at the same time, the temperature at the outlet of the evaporator (connection 23) does not change linearly with the return

temperatures. Therefore, the heat supply from the GTD well does not show a linear behavior, too. The same applies to the HT-ATES, where the combination of an increase in flow and a decrease in the temperature going into the HT-ATES result in a non-linear progression. These characteristics are not seen in option 1 as the flow through the evaporator also increases with the return temperatures and the temperature at the outlet of the evaporator thus shows a linear trend (see Figure 50 in Appendix C).

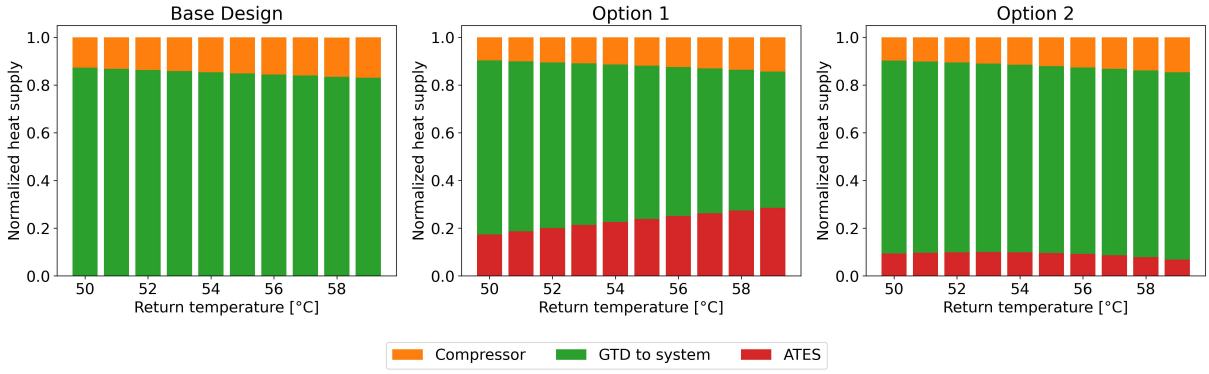

Figure 25 Influence of return temperature on distribution of energy delivery during one hour at medium demand

In general, it can be stated that lowering the return temperatures leads to a lower COP for the heat pump but an increase in the combined thermal energy supply from the HT-ATES and the GTD well. Therefore, considerations to switch the positions of TUD and OWD in the system to use the higher return temperatures of TUD to achieve a better COP of the heat pump, would ultimately reduce the thermal energy supply from the GTD well. During peak demands, this would result in an increase in the WKC heat supply and in GHG emissions.

The impact of reducing the return temperature on a full year simulation is shown in Figure 26. The return temperatures of TUD and OWD were each reduced by 2.5°C and 5°C. In all options, the proportion of the GTD well supply increases for lower return temperatures. While there is a slight increase in the share of the HT-ATES, it is almost too small to be seen in the plot. On one hand, the cut-off temperature of the HT-ATES is reduced with lower return temperatures. Moreover, if the flow rates in the system are decreased, more flow is available to load the HT-ATES. This is seen in an increase of the thermal energy loaded from the GTD well to the HT-ATES. On the other hand, the reduced flows in the system also lead to less flow to discharge the HT-ATES and a decrease in the thermal energy extracted from the HT-ATES.

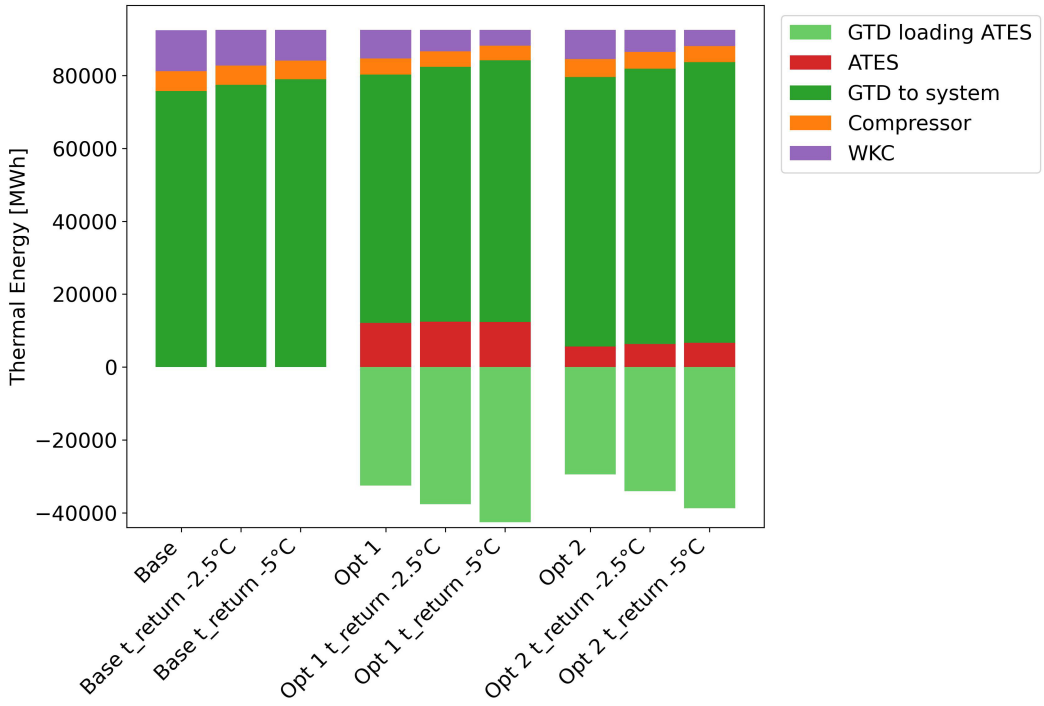

Figure 26 Annual thermal energy per heat source for reduced return temperatures

Table 8 summarizes how reducing the return temperature affects the PIs in design option 1. The results for the base design and design option 2 are shown in Table 16 and Table 17 in Appendix C. For a reduction of 5°C, the GHG emissions measured in terms of the proportion of the WKC are reduced by 45% in design options 1 and 2, and 25% in the base design. The SCOP of the heat pump slightly decreases due to the lower return temperatures. The electricity consumption of the compressor and the GTD well pump both decrease due to the lower flow rates in the system. In contrast to the heat pump SCOP, the system SCOP increases. As considerably more thermal energy is injected into the HT-ATES, the recovery efficiency decreases for reduced return temperatures.

Table 8 Performance indicators for design option 1 for reduced return temperatures

Performance Indicator	**Reduction of Return Temperature**		
	Base Case	**- 2.5°C**	**- 5°C**
Annual GHG emissions • Q WKC [MWh]	7 769	5 820	4 283
Annual Electricity consumption • W Compressor [MWh] • W GTD well pump [MWh]	 4 452 8 001	 4 231 7 915	 4 042 7 850
SCOP Heat pump [-]	5.33	5.13	4.95
SCOP System [-]	6.41	6.76	7.06
η_{th} HT-ATES [-]	0.37	0.33	0.29

3.2.4 Increasing Heat Demands

In the following analysis, two adjustments to the demand data are examined: first, a general increase of 50% in both TUD and OWD demands; second, an increase in OWD demands coupled with a decrease in TUD demands.

An increase in the heat demands without changing the supply and return temperatures will lead to higher flow rates in the system. In the current setup, the GTD well runs at full capacity whenever the total flow of TUD and OWD exceed 375 m³/h. Beyond that, the additional flow is directed through the HT-ATES if the hot well is above the cut-off temperature. When even the flow limit of the HT-ATES is exceeded, the bypass in the system is needed. As seen in Figure 27, when discharging the HT-ATES, the flow limit is not reached yet, especially in spring and autumn. By increasing the demands in the system, this additional capacity could be used.

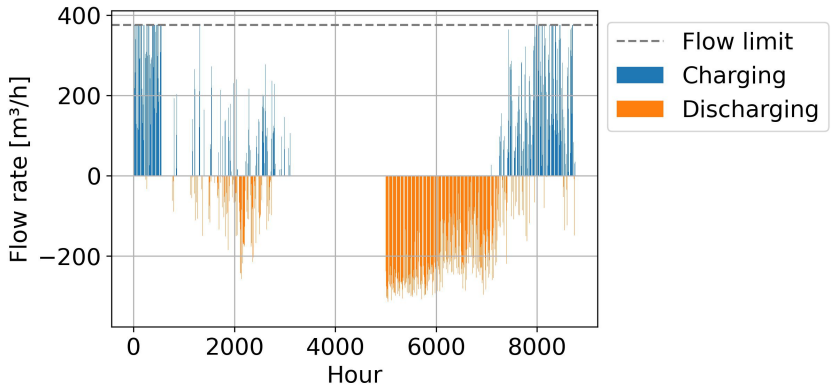

Figure 27 Flow rates in the HT-ATES for regular demands

To accommodate the additional demands, the model is run with a condenser capacity of 10 MW. The results of the model with demands increased by 50% is presented in Figure 28. It is seen that increasing the demands increases the proportion of thermal energy supplied by the GTD well, the heat pump and the WKC, but decreases the proportion of thermal energy supplied by the HT-ATES. By increasing the flows in the system, the HT-ATES is discharged with higher flow rates but also loaded with lower flow rates. While for regular demands, the HT-ATES is loaded with flow rates up to 300 m³/h (see Figure 27), with increased demands, the flow rates while loading the HT-ATES are lower (see Figure 29). Therefore, the total volume of the hot well is smaller at the end of the loading period, the hot well temperatures decrease faster, and the cut-off temperature is reached earlier. In other words, the storage is depleted faster. In the GTD well, the extraction temperature is constant at 74.5°C and extracting more from the GTD well does not reduce the geothermal capacity in the short term.

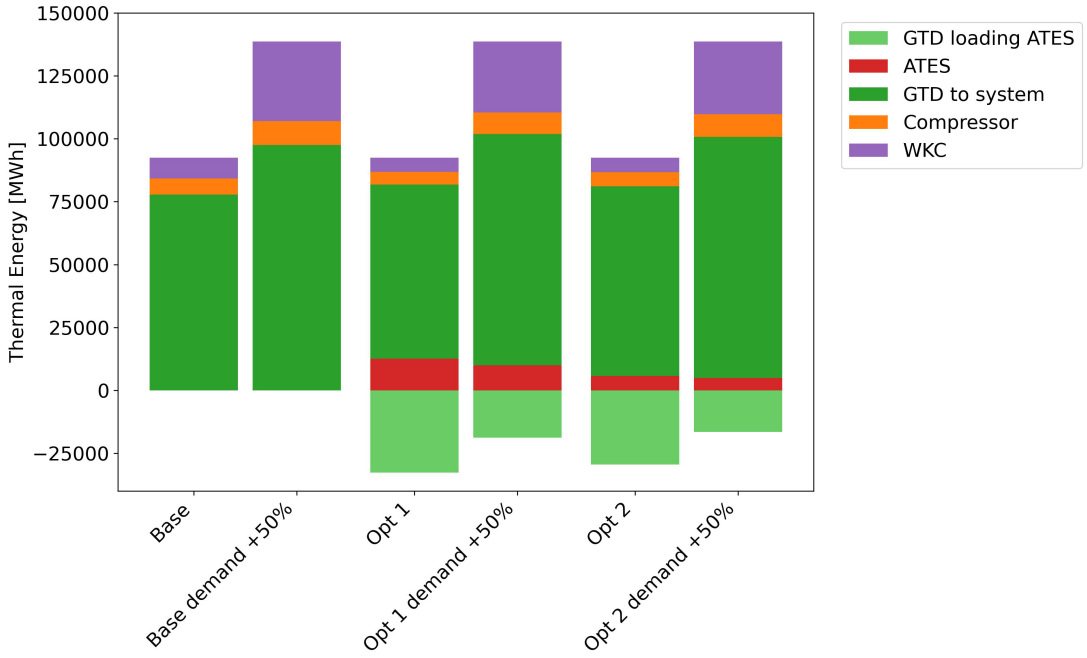

Figure 28 Annual thermal energy per heat source for demands increased by 50%

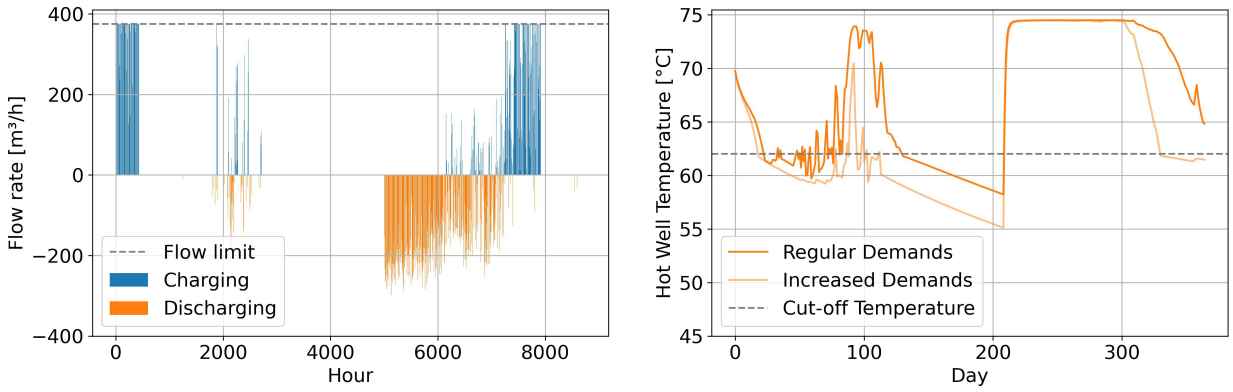

Figure 29 Flow rates and hot well temperatures of the HT-ATES with demands increased by 50%

Although the OWD network is expected to expand in the future, the demands for TUD are anticipated to decrease due to the modernization of buildings. In the projection for the year 2042, known as 'scenario 4', OWD demands are projected to increase by 300%, while TUD demands are expected to decrease by 55%. Scenario 4 was simulated with a 10 MW condenser. As previously explained, higher flow rates enable more discharging of the HT-ATES but also result in less available flow for loading it. To sufficiently load the HT-ATES, the loading period was extended in scenario 4 to begin in May. The results for scenario 4 are shown in Figure 30.

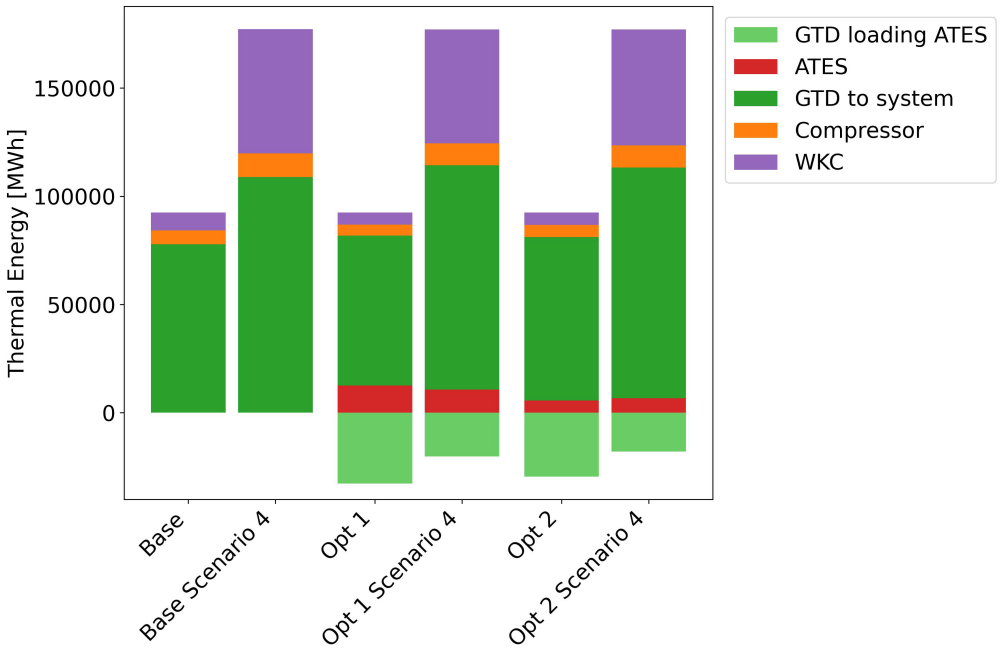

Figure 30 Annual thermal energy per heat source for 'scenario 4'

Even with an extended loading period, the absolute thermal energy supplied by the HT-ATES decreases for option 1. In option 2 however, the heat supply from the HT-ATES slightly increases. Again, the flows to charge and discharge the HT-ATES as well as the hot well temperatures are the same in option 1 and option 2. However, the cold well temperatures differ and therefore also the thermal energy extracted from the HT-ATES (see Figure 31). Especially during cold outside air temperatures, OWD has lower return temperatures than TUD. In both options, due to the increased flows of OWD and the reduced flows of TUD, the mixed return temperature of both consumers tends to be lower than for regular demands.

In option 1, this leads to lower temperatures going into the evaporator (connection 21). At the same time, during peak demands when the condenser operates at maximum capacity, increased flows lead to smaller temperature drops at the evaporator between connections 21 and 22. As shown in Figure 31, the cold well temperatures thus are approximately the same for regular demands and scenario 4, especially in the first 150 days of the year. Then, the temperatures change because of the different loading periods. The hot well temperatures again drop faster than for regular demands due to the increased flow rates (see Figure 51 in Appendix C). This means that overall, even with an increased loading period, the thermal energy supplied by the HT-ATES is less in scenario 4 than for regular demands.

In option 2, the hot well temperatures are the same as in option 1. However, scenario 4 leads to lower temperatures going into the bypass and the HT-ATES without passing the evaporator. This is seen in the reduced cold well temperatures compared to the regular demands (Figure 31). Therefore, scenario 4 leads to an increase in the thermal output of the HT-ATES in option 2.

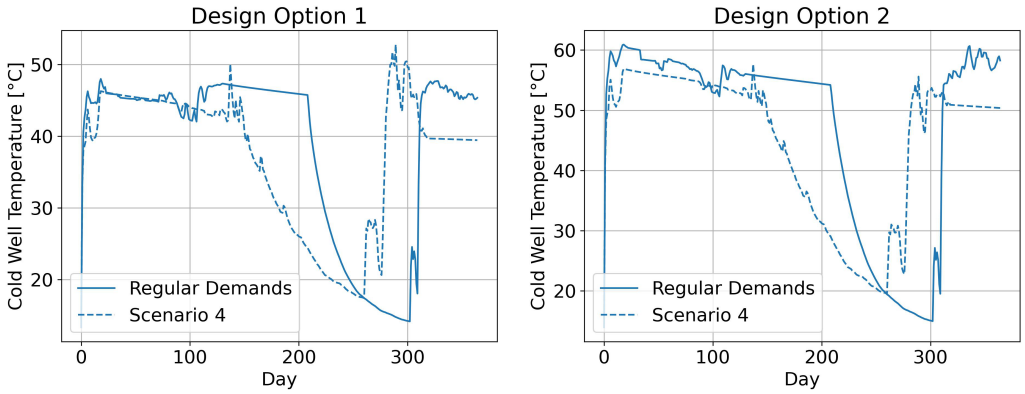

Figure 31 Comparison of cold well temperatures for 'scenario 4'

The PIs for the scenario with the demands increased by 50% and scenario 4 are compared to a regular demand scenario with a 10 MW condenser capacity in Table 9. Again, only the results for option 1 are shown, for the base design and design option 2, see Table 18 and Table 19 in Appendix C. Increasing the demands leads to more GHG emissions and an increase in the electricity consumption of the system. Overall, the heat pump SCOP and the system SCOP slightly decrease. As explained before, these values also depend on the flow rates in the system which affect the electricity consumption of the compressor. For higher demands, the flow rate in the system increases. However, the flow that can be directed through the evaporator is limited. Therefore, the flow rate and temperature difference at the evaporator change with increased demands. The recovery efficiency of the HT-ATES increases, as less thermal energy is injected into the HT-ATES.

Table 9 Performance indicators for design option 1 for increased demand scenarios

Performance Indicator	**Increasing the demands**		
	Regular demands (10 MW Condenser)	**+ 50%**	**'Scenario 4'**
Annual GHG emissions • Q WKC [MWh]	5 565	28 232	52 707
Annual Electricity consumption • W Compressor [MWh] • W GTD well pump [MWh]	 5 060 8 024	 8 587 8 537	 9 959 9 955
SCOP Heat pump [-]	5.17	4.62	4.54
SCOP System [-]	6.25	5.97	5.73
η_{th} HT-ATES [-]	0.39	0.53	0.53

3.2.5 Reducing Pump Rates of GTD Well

As introduced in the methodology section, the power consumption of the circulation pump in the GTD well is notably high and therefore reducing the flow rate in the GTD well can have a significant impact on the overall energy efficiency. Figure 32 shows the power consumption of the pumps in the GTD well and the HT-ATES for the base design as well as the design options with HT-ATES. As the same flow rates apply for option 1 and 2, the circulation pumps perform equally in both HT-ATES options. It is seen that during the operation period of the HT-ATES, the pump rate of the GTD well is constantly at 375 m³/h resulting in a power consumption of approximately 1.13 MW. During this period, the GTD supplies heat to TUD

and OWD and loads the HT-ATES at the same time. In the base design, the pump rate of the GTD well varies and depends only on the summed flow rate of OWD and TUD. When the HT-ATES is shut down, the pump rates are the same in all options. The circulation pump of the HT-ATES has a much lower power consumption with a maximum of 0.08 MW. The cumulative of the power consumption shows the total annual energy consumption. Without HT-ATES in the system, a total energy consumption of 5500 MWh is needed per year to run the GTD well. The loading of the HT-ATES results in an additional 2450 MWh per year neglecting the power consumption of the HT-ATES circulation pump.

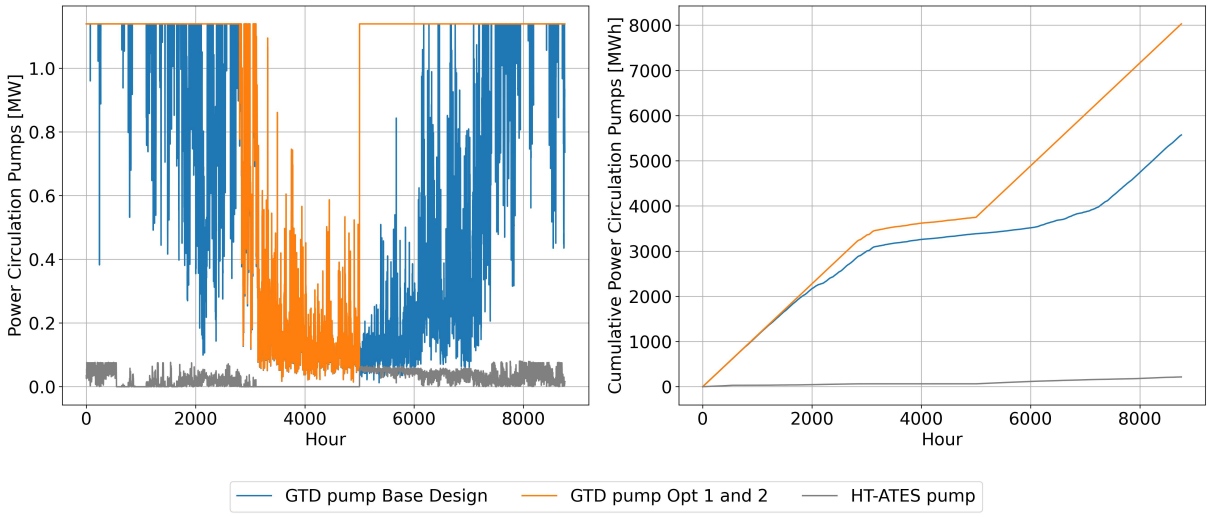

Figure 32 Power consumption of the circulation pumps in the system

Based on these results, two considerations to improve the overall efficiency of the system are investigated:

1. *Merit order of GTD well and HT-ATES:* In the current set-up, the GTD well supplies at its maximum flow rate of 375 m³/h during medium and peak demands. The additional flow available in the network is directed through the HT-ATES, also up to a maximum flow rate of 375 m³/h. It is analyzed whether operating the GTD well at a lower flow rate and increasing the flow rates in the HT-ATES instead reduces the total power consumption in the system.
2. *Loading strategy for HT-ATES:* The starting date to load the HT-ATES in summer is chosen as late as possible such that the needed volume in the hot well is achieved but the heat losses in the HT-ATES are as low as possible. Therefore, the flow rate to load the HT-ATES and consequently of the GTD well is maximized. An alternative to be examined is to load the HT-ATES at a lower GTD pump rate but over a longer period tolerating higher heat losses in the hot well.

Merit order of GTD well and HT-ATES

If the total flow in the system is lower than the combined maximum flow rates of the GTD well and the HT-ATES (750 m³/h in total), it can be adjusted how to split the flow rate between the GTD well and the HT-ATES. If more flow is directed through the HT-ATES, more additional thermal energy is needed from the WKC, as the hot well temperatures are usually lower than the GTD well. The more flow is directed through the GTD well, the more electricity is needed for the GTD well pump.

Figure 33 shows the total power consumption of the WKC and the GTD pump depending on how the total flow rate in the system is split between the GTD well and the HT-ATES. The left plot shows the power consumption of the WKC and the GTD pump separately while the right plot shows the sum of both. The results are shown for an exemplary peak demand situation of 20 MW, 10 MW for TUD and OWD respectively and a required supply temperature of 85°C. The power consumption of the GTD pump is 0 if all flow is directed through the HT-ATES and no flow goes through the GTD well (left side of the plots). Following the pump characteristic as shown in Figure 13, the power consumption of the pump grows exponentially with the flow rate in the GTD well. In contrast, the more flow is directed through the GTD well, the less additional energy is needed from the WKC.

The extraction temperature from the GTD well is constant at 74.5°C while the hot well temperature of the HT-ATES varies over the year. Therefore, a set of curves is shown for different hot well temperatures. The lower the temperatures in the HT-ATES, the more thermal energy is needed from the WKC. The absolute energy provided by the WKC as shown in the plots is only representative for the given input and depends on the demands. In the right plot, it is seen that the minimum of the total power consumption shifts towards the right for lower hot well temperatures. For a hot well temperature of 76°C which is higher than what the GTD well provides, it would be most efficient to direct all flow through the HT-ATES. For hot well temperature between 68-70°C, splitting the flow equally between HT-ATES and GTD well is optimal. For lower hot well temperatures, the power consumption of the WKC exceeds the power consumption of the GTD pump and all flow should be directed through the GTD well.

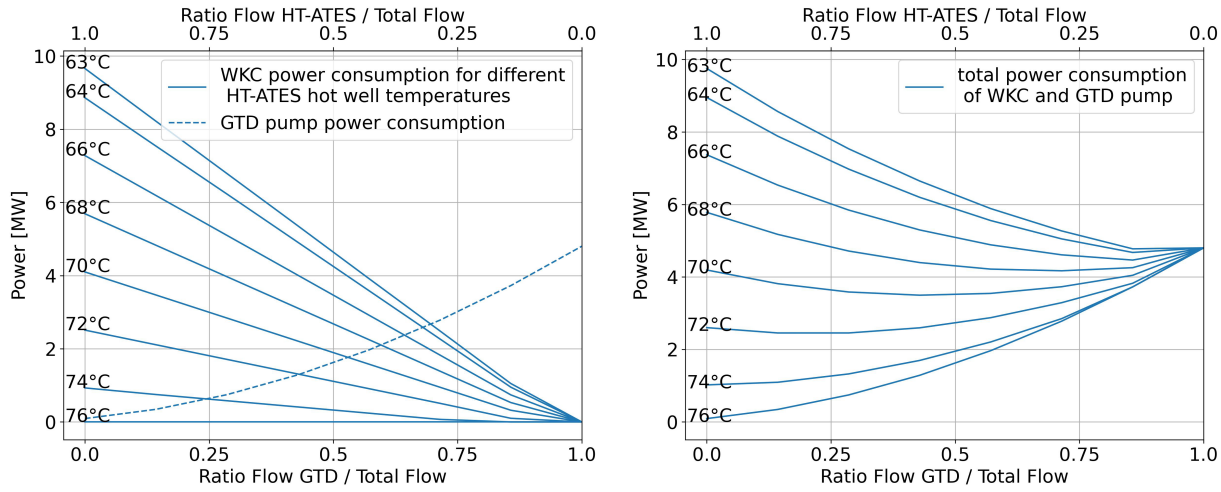

Figure 33 Power consumption of GTD well pump and WKC depending on flow ratio between GTD and HT-ATES

The limitations of the flow rates in the system are not considered in Figure 33. The total flow rate in the system for the given input is 600 m³/h. Therefore, directing all flow through either HT-ATES or the GTD well is not feasible. When considering only the feasible flow ranges, the results are as shown in Figure 34 but the dynamics are still the same. Reducing the flow rate in the GTD well and simultaneously increasing the flow rate in the HT-ATES, can be considered for hot well temperatures above 70°C. With the given data set, this is only the case at the end of the summer loading period in November and for a short time in April (see Figure 19). Especially in the first years of operating the HT-ATES, the temperatures and volume of the hot well will vary whereas the GTD well will provide a constant hot temperature. Therefore, ranking the GTD well first in the merit order is currently considered

the best option. However, in future scenarios the temperatures in the hot well could be increased for example by converting surplus electricity on campus into thermal energy.

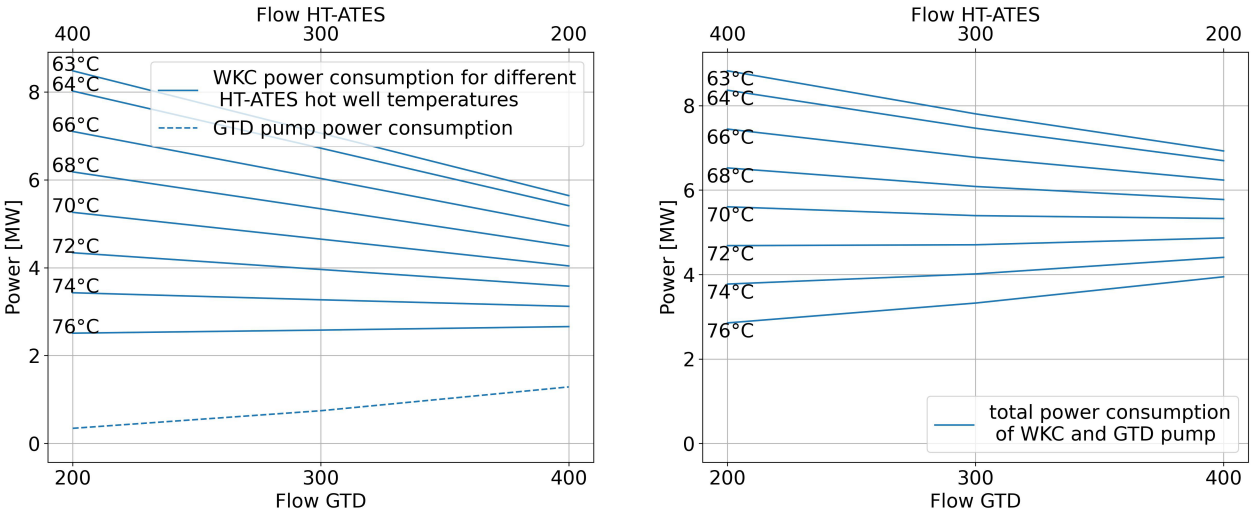

Figure 34 Power consumption of GTD well pump and WKC for feasible flow ranges

In the figures above, the minimum total power consumption of WKC and circulation pumps is considered as optimum. However, the energy source for the WKC is gas while the circulation pumps are powered by electricity. If this electricity is considered to be from renewable sources and the goal is to minimize GHG emissions, running the GTD well at maximum capacity is the best option for any given hot well temperature. This is true for peak demands, where the heat pump runs at full capacity and the WKC is needed. In a medium demand scenario, the WKC is turned off and the heat pump runs in part load. Then, an increase in the flow rate of the GTD well reduces the thermal output of the condenser and consequently the power consumption of the compressor. As the compressor is powered by electricity too, an optimization is then in any case based on reducing the total power consumption.

Loading Strategy for HT-ATES

The results presented thus far are based on a summer loading period of the HT-ATES starting from the beginning of August with a flow rate of 365 m³/h in the GTD well. As an alternative, a loading strategy with a lower flow rate but starting from beginning of May is analyzed. To make the two strategies comparable, a flow rate of 260 m³/h in the GTD well is needed during the longer loading period to still reach the same volume of 500 000 m³ in the hot well in November. This means that the HT-ATES is loaded with a flow rate according to the difference between 260 m³/h and the required flow rate to meet the demands of the consumers (see Figure 35). Choosing an even lower flow rate in the GTD well would result in a smaller hot well volume or – if the flow rate to load the HT-ATES is set to a fixed value – increase the thermal energy supply needed from the heat pump to meet the demands of the consumers.

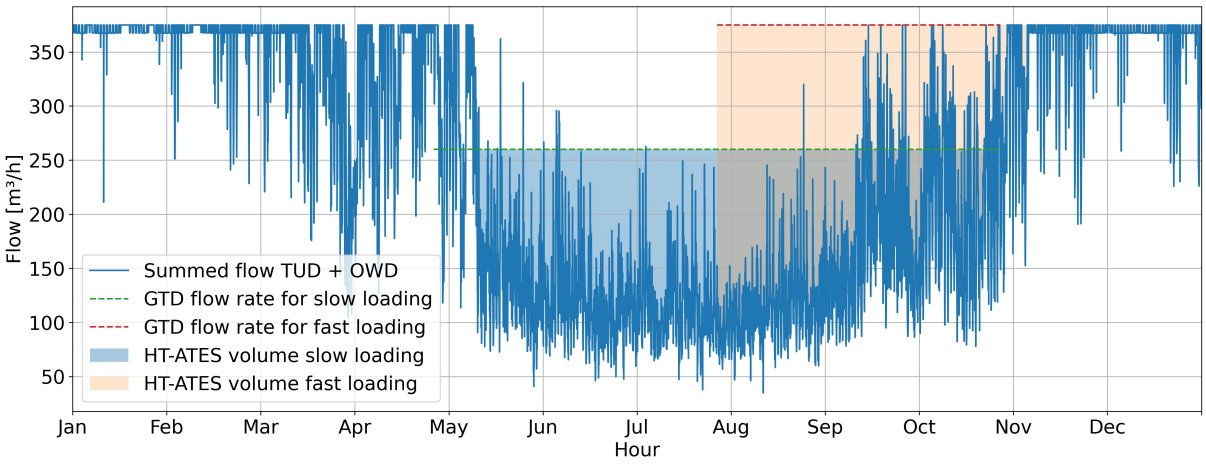

Figure 35 Two different loading strategies for HT-ATES

The volume and temperatures of the HT-ATES as well as the cumulated power needed for the GTD well pump for the two loading strategies is shown in Figure 36 and Figure 37. To see the effect on a full year, the cycle is started with the loading period in May. The volume in the hot well increases with a lower gradient and the temperatures at the end of the loading period decline slightly faster than for the fast loading strategy. Even though the heat is stored for a longer period when loading the HT-ATES slowly, the temperature difference in the hot well during discharging is relatively small. The thermal recovery efficiency is 0.20 for the slow loading strategy and 0.22 for the fast loading strategy. Loading the HT-ATES slowly results in a reduction of approximately 600 MWh in the GTD well pump's power consumption, which is 7.3% of the annual power required for the fast loading strategy.

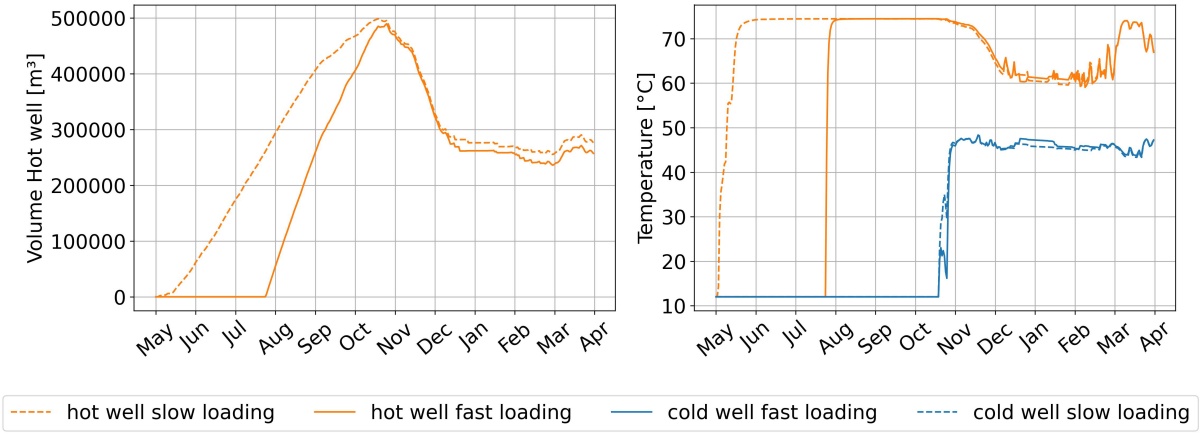

Figure 36 Comparison of volume and temperature of the HT-ATES for different loading strategies

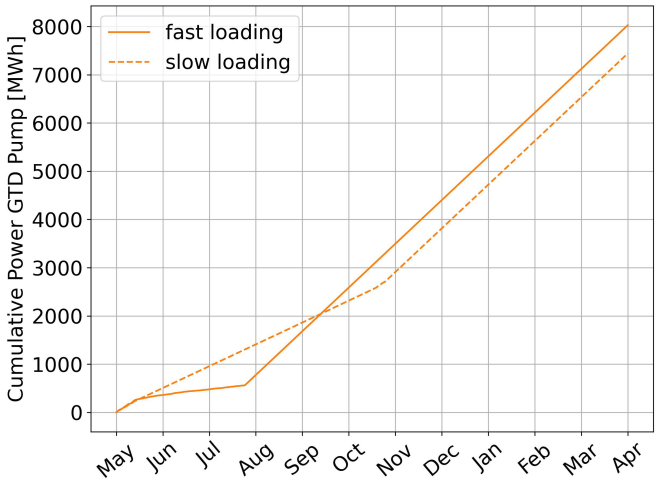

Figure 37 Comparison of GTD well pump power consumption for different HT-ATES loading strategies

4 Discussion

4.1 Differences Between the Design Options

Two options to integrate the HT-ATES into the heating system were modeled and compared to a reference design without HT-ATES. It was shown that the options with HT-ATES can improve the system by reducing the heat supply from the WKC if the hot well temperature is above the return temperature of the consumer. This definition of the cut-off temperature becomes more comprehensible in a schematic representation of one hour at peak demand as shown in Figure 38, in which option 1 is compared to the base design.

Figure 38 shows step by step how the flow rate for a given thermal energy demand is directed through the system. Each component in the system can raise the temperature of that flow to a certain level. The figure shows how the combination of flow rate and temperature level defines the proportion of each heat source for one hour of the demand data set.

Step 1: Evaporator

The heat demand in the system is represented as the orange rectangle of which the size is defined by the needed flow, and the supply and return temperatures of the heat sink. Once the model has solved the system, this rectangle has to be fully covered by the thermal energy provided from the heat sources. TUD and OWD are simplified as one consumer. Starting at the outlet of the heat sink, the flow in the system has a temperature level that is equal to the return temperature of the consumer. In the base design, part of the flow is directed through the evaporator (375 m³/h) corresponding to the flow limit of the GTD well and the rest of the available flow in the system through the bypass.

In option 1, the flow through the evaporator is doubled (750 m³/h) according to the flow limits of the GTD well and HT-ATES taken together. The size of the rectangle representing the evaporator is the same in both the base design and option 1 and is defined by the capacity of the condenser and the COP of the heat pump. Therefore, the temperature at the outlet of the evaporator (the lower edge of the blue rectangle) is lower in the base design than in option 1.

Step 2: GTD well and HT-ATES

After the evaporator, the HT-ATES and the GTD increase the temperature level to the temperatures in the hot well and in the GTD respectively. In the base design, only 375 m³/h are raised to the GTD well temperature (74.5°C). In option 1, the HT-ATES additionally heats up 375 m³/h to the temperature level of the hot well.

Step 3: Heat pump

Once the flow has passed the GTD well and the HT-ATES, it is directed through the condenser. The condenser adds the same amount of thermal energy in both design options, which is the area of the evaporator rectangle plus the energy supplied by the compressor.

Step 4: WKC

The share of energy supplied by the WKC is shown in the plot on the bottom. The WKC provides the residual of the demand that has not been covered by the heat pump, GTD and HT-ATES.

Option 1(B) shows the proportion of each heat source when the HT-ATES is operated at hot well temperatures below the return temperature of the consumer. In this case, the flow that is directed through the HT-ATES is only heated up to a temperature level below the return temperature. The rectangle representing the WKC then has to cover a larger area than in the base design. Therefore, the cut-off temperature has to be set to the return temperatures of the consumer.

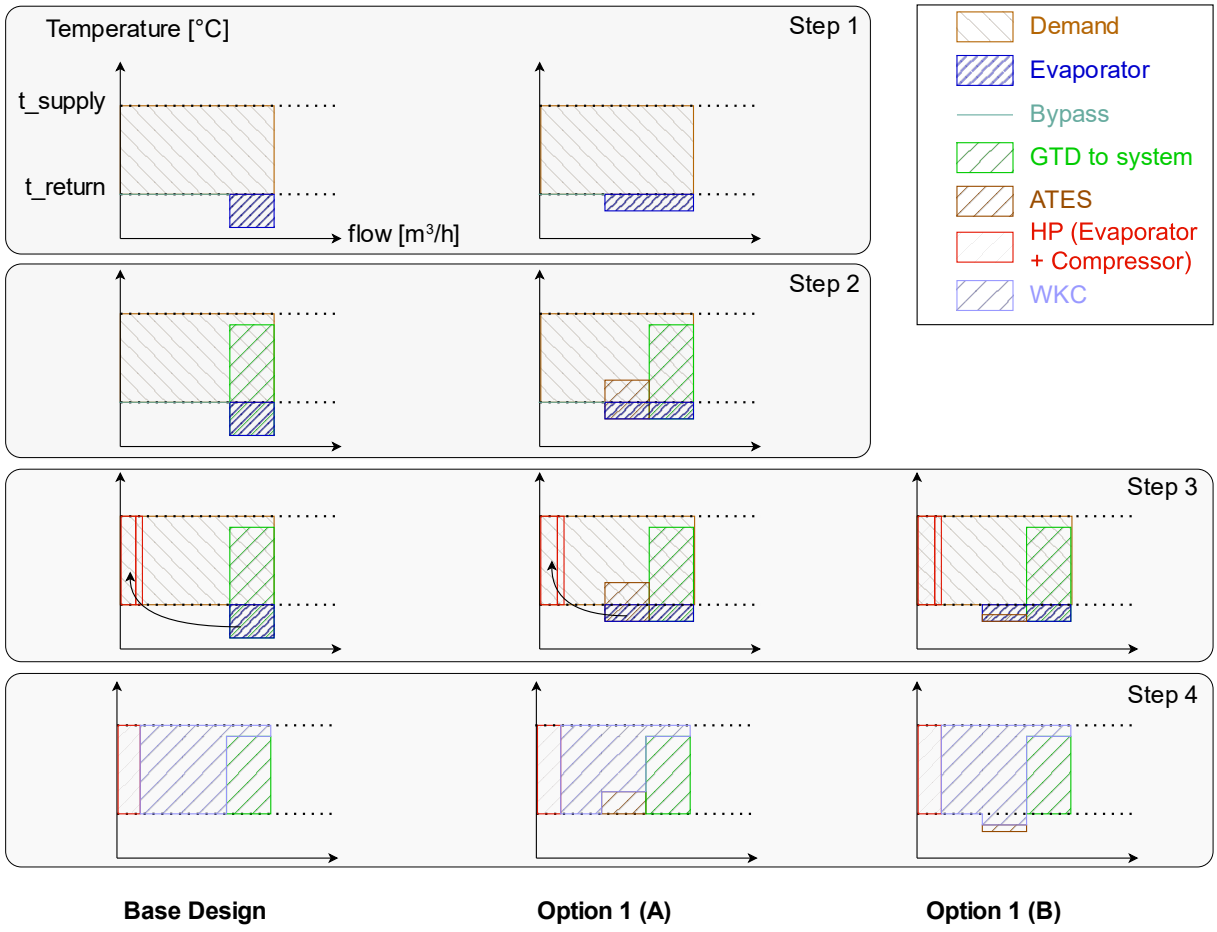

Figure 38 Schematic representation of the heating system with and without HT-ATES

Using this schematic representation, the main differences between option 1 and option 2 can be explained as well. If the cut-off temperature of the HT-ATES is set to the return temperature of the consumer, the HT-ATES can be connected directly behind the consumer (option 2) instead of behind the evaporator (option 1). As seen in Figure 39, the thermal output of the evaporator is the same in both options, but the flow through the evaporator is again limited to 375 m³/h in option 2. Therefore, a lower temperature level is reached at the outlet of the evaporator in option 2 and the thermal energy supply of the GTD well is greater than in option 1. On the other hand, when the HT-ATES is connected behind the evaporator, the lower temperatures used to extract heat from the HT-ATES result in a greater thermal energy supply from the HT-ATES in option 1.

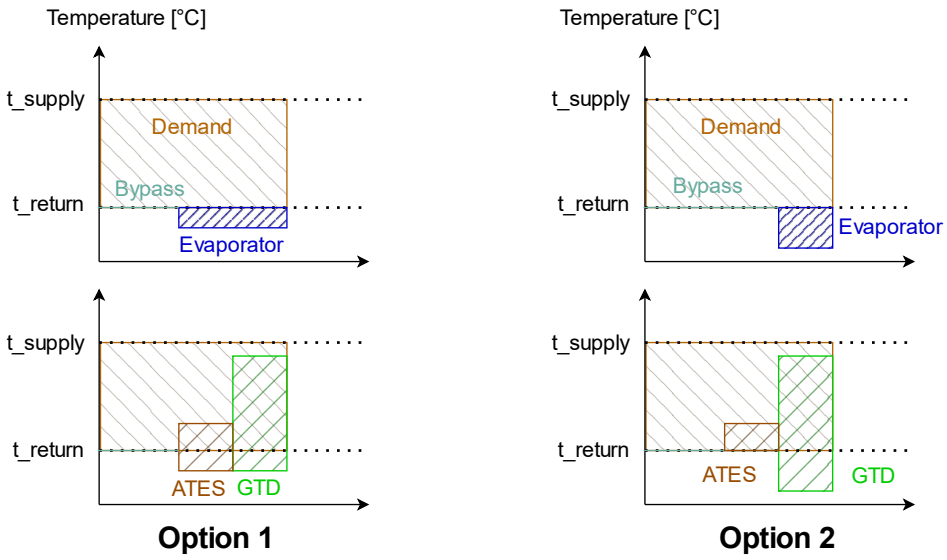

Figure 39 Schematic representation of option 1 and option 2

Sizing the Heat Pump

For all options it was shown that increasing the size of the condenser results in a higher share of the GTD well in the thermal energy supply. The more thermal output is supplied to the system at the condenser side, the more thermal output is extracted at the evaporator side and the lower is the temperature used to extract heat from the GTD well. In option 1, the size of the condenser is also linked to the thermal energy that can be extracted from the HT-ATES, while in option 2, the HT-ATES is independent of the heat pump size. Consequently, in option 1, the temperatures of the cold well decreased slightly with an increase of the condenser size. The volume of the hot and cold well was not affected by the size of the condenser as it only depends on the total flow rates in the system which are defined by consumer demands and required temperatures.

The results of the model for different condenser sizes have shown that a condenser with 8 MW capacity would be sufficient to cover 85% of the annual demand with renewable heat sources in all design options (see Figure 18). With the HT-ATES, this aim is even reached with a 6 MW condenser. However, the actual performance of the heat pump highly depends on the specific heat pump model and its attributes such as the working fluid and the size of the heat exchanging areas in the evaporator and condenser. Furthermore, given that demands in the network will increase in the future, the design of the heat pump should include provisions for additional capacities. If possible, the condenser size could be increased later on by adding units to the heat pump. Alternatively, the heat pump might need to be oversized initially to fit the anticipated future demands. This consideration will influence both the initial investment and the long-term adaptability of the system.

4.2 Evaluation of System Performance

Evaluating the design options based on the PIs showed that option 1 scored the best (see Table 5). With a cut-off temperature of 61°C and the condenser capacity set to 8 MW, a reduction in GHG emissions of 31% in option 1 and 29% in option 2 was achieved compared to the base design. Option 1 showed a better $SCOP_{HP}$ than option 2. This was explained with the higher flow rates in the evaporator in option 1. In option 2, the flow entering the evaporator is primarily covered by the return flow from OWD. In option 1, flows from TUD are

added as the flow rate limitation is higher in the connection to the evaporator. As the return temperatures of TUD are usually higher than the return temperatures of OWD, the $SCOP_{HP}$ is slightly better in option 1. This in turn influences how much thermal energy is extracted at the evaporator. A better COP for the heat pump leads to higher thermal outputs at the evaporator and therefore more heat supply from the GTD well in option 1 than in option 2.

In line with the results for the $SCOP_{HP}$ and the GHG emissions, option 1 also has the lowest electricity consumption for the compressor. Therefore, option 1 also had a better $SCOP_{System}$ than design option 2. Nevertheless, the base design has the best system SCOP. This is because the loading and discharging of the HT-ATES significantly increases the pump rate in the GTD well and therefore the electricity consumption in the system.

Regarding the evaluation of HT-ATES efficiency, option 1 had a thermal recovery efficiency of 0.37 and therefore scored better than option 2 with 0.19. The higher thermal recovery efficiency is due to the lower temperatures used to extract thermal energy from the HT-ATES. Even though less thermal energy is extracted from the HT-ATES in option 2, the injected thermal energy is the same in both options with HT-ATES as the injected flow rates and temperatures do not differ. Therefore, the electricity consumption of the GTD well pump was the same in both options with HT-ATES.

The PIs used in this study do not account for certain aspects that are relevant when evaluating such a system. Below, additional aspects that could not be assessed qualitatively using the results of the computational model are elaborated.

Financial Evaluation

When financially evaluating a project, both capital expenditure (CAPEX) and operational expenditure (OPEX) are critical factors to consider. CAPEX includes initial investment costs such as acquisition of technical equipment and installation costs for drilling of the wells. Also, obtaining necessary permits could fall into this category. OPEX involves ongoing costs like energy expenses and maintenance of the system.

Comparing only the two design options with HT-ATES, no difference can be made regarding the CAPEX. Both design options require the same investment for installation of the GTD well and HT-ATES system. The base design has the lowest CAPEX, as no HT-ATES system is installed.

Regarding the OPEX, energy costs for electricity and gas consumption should be taken into account. The energy costs were estimated with an electricity price of 0.31€ per kWh and a gas price of 1.32€ per m³ (Overstappen, 2024). Using a conversion of 10 kWh for 1 m³ of gas, the results are as presented in Table 10. In design options 1 and 2, the same flow rates apply in both the GTD well and the HT-ATES. Therefore, the energy expenses for running the circulation pumps are the same. The difference in the thermal output is only due to different injection temperatures. Due to a better COP of the heat pump, option 1 has a slightly lower annual electricity consumption for the compressor than option 2. The base design has the lowest electricity consumption, but the highest gas consumption. All in all, the energy costs are in the same order of magnitude for all design options. Slightly higher energy costs can be expected for design option 2. Considering both CAPEX and the OPEX, it is worth noting that the base design likely has the lowest overall costs.

Table 10 Estimated energy costs for each design option based on the model results as shown in Table 5

	Base Design	Option 1	Option 2
Annual Gas consumption			
• Q WKC [*k*€]	1 488	1 026	1 051
Annual Electricity consumption			
• W Compressor [*k*€]	1 697	1 380	1 522
• W GTD well pump [*k*€]	1 688	2 489	2 489
Total	4 873	4 895	5 062

Besides the expenditure associated with the project, revenues that will be generated from the thermal energy production have to be included in the financial evaluation. On one side, the heat delivered to TUD and OWD will be sold at the current heat price. On the other side, the renewable energy generation will be subsidized (Bloemendal et al., 2021). As the model in this study is designed to cover a given annual heat demand, the amount of heat that is sold will be the same in all design options. The subsidies relate to the thermal energy produced by the GTD well. More specifically, the total thermal energy that is produced is relevant. This means, that also the thermal energy loaded from the GTD well into the HT-ATES is subsidized, even if the HT-ATES has a low thermal recovery efficiency. Therefore, both options with HT-ATES will receive significantly more subsidies than the base design. Option 2 will secure the highest subsidy as it has the highest thermal output from the GTD well (see Table 4).

In addition to the fixed expenditures, the system can be further optimized to save costs. For example, the electricity price can vary significantly over time depending on the demand and the availability of (renewable) energy sources. The system could respond to these variations by scheduling the loading of the HT-ATES accordingly. Loading the HT-ATES mainly increases the pump rate of the GTD well pump and should therefore take place during periods of low electricity prices. Moreover, the concept of ‘Power to Heat’ could be applied where electrical power is converted to thermal energy. In this way, additional thermal energy could be stored in the HT-ATES when electricity prices are low.

Impact of the HT-ATES on the Subsurface

Besides the positive effect of reducing GHG emissions, the environmental impact of a HT-ATES system on the subsurface should not be neglected. In design option 1, the initial groundwater temperature of approximately 12°C is increased to 74.5°C in the hot well and 50°C in the cold well. In design option 2, the cold well even reaches temperatures of 60°C. These temperature changes can lead to precipitation or dissolution of minerals in the aquifer and cause effects on the groundwater ecosystem. Although this study does not focus on these effects, it can be stated that minimizing subsurface disturbance results in a lower environmental impact.

The design options with HT-ATES do not differ in terms of the storage volume of the HT-ATES. The volume is determined by the system's flow rates, which are influenced by demand, supply and return temperatures. However, the lower temperatures of the cold well in option 1 can be seen as a reduced impact on the subsurface compared to design option 2.

Sustainable Use of the GTD well

Regarding the GTD well, the operational lifespan is a key parameter for measuring sustainability. In general, geothermal energy is classified as a renewable energy due to the inexhaustible amount of stored heat and a continuous reproduction through radioactive decay (Axelsson, 2012). A geothermal system consists of an injection well and an extraction well. The cooled down fluid that is injected into the cold well forms a cold front that continuously moves and eventually reaches the extraction well. This is called the thermal break-through and marks a point in time, when the production temperature of the geothermal well drops. A thermal break-through can lead to the need to shut down the system if the production temperature is too low. By allowing the system to rest, thermal recovery of the reservoir is possible but is associated with financial losses (Fadel et al., 2022).

Balancing recharge and discharge of the GTD well leads to a sustainable operation of the system. The later the thermal break-through occurs, the longer the well can be operated, which is desirable, not least for financial reasons. For the system on TUD's campus, no information is given on the recovery rate of the GTD well. However, the proposed design options differ in terms of the annual thermal energy production of the GTD well. The two design options with HT-ATES require more thermal energy from the GTD well, potentially reducing its longevity. In design option 1, adding the HT-ATES results in an annual thermal output of approximately 100 GWh from the GTD well. Design option 2 requires an additional 3 GWh per year, which could further reduce the life expectancy of the GTD well compared to option 1.

4.3 Possibilities to Improve System Performance

The robustness of the system was assessed by adjusting several parameters and settings in the model. It was shown that the different design options respond differently to these adjustments.

In terms of reducing GHG emissions, lowering the return temperature had the most significant impact on the system's performance. The governing effect is that with lower return temperatures also lower temperatures can be used to discharge both the HT-ATES and the GTD well. A 5°C reduction resulted in a 45% decrease in thermal energy supply by the WKC in both HT-ATES design options and 25% in the base design. Compared to the base design, the reduction of GHG emissions is more pronounced in the options with HT-ATES, because reducing the return temperatures also reduces the cut-off temperature of the HT-ATES.

Regarding the performance of the heat pump, reducing the supply temperature leads to a better $SCOP_{HP}$ while reducing the return temperature adversely deteriorates it. Moreover, when reducing the supply temperatures, the heat pump can be shut down when the supply temperature is below the GTD well temperature and the flow rates in the system are low. Also, the flow rates in the system are affected differently. Reducing the supply temperature leads to an increase in the total flows and therefore more available flow to discharge the HT-ATES during medium demands. In contrast, reducing the return temperatures decreases the total flow in the system and less flow can be used to discharge the HT-ATES. In contrast to the $SCOP_{HP}$, the system SCOP improves for both a reduction of the supply and of the return temperatures.

In order to improve the performance of the HT-ATES, it was investigated whether increasing the demands and therefore the flows in the system would lead to more thermal output from

the HT-ATES. However, it was shown that higher flow rates also caused the cut-off temperature to be reached sooner compared to the regular demand scenario. Moreover, if the flow rates in the system are higher, more flow is available to discharge the HT-ATES but also less flow is available to load the HT-ATES during summer as long as the GTD well is prioritized in the merit order. In the current set-up, the flow rates in the HT-ATES are not directly set but depend on the flow rate as defined by the demands in the system. This is explained in Figure 40. When the HT-ATES is discharged and the available flow in the system is above 375 m³/h, the GTD well is run at full capacity and any additional flow is directed through the HT-ATES. During loading periods, the flow rate in the HT-ATES is set such that the GTD well runs at full capacity. It then covers the heat demand and loads the HT-ATES at the same time.

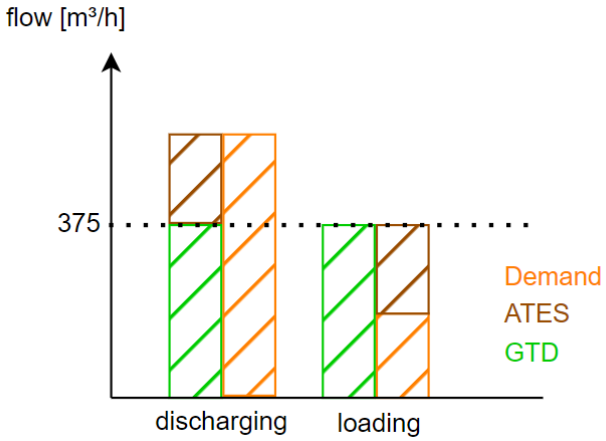

Figure 40 Schematic representation of flow rates in the HT-ATES

Additionally, a future demand scenario (‘scenario 4’) in which OWD demands increase and TUD demands decrease was modeled. In all design options, the heat supply from the GTD well, the heat pump and the WKC increased for this scenario. However, it was observed, that in option 1, the share of thermal energy supplied by the HT-ATES decreased while it increased in option 2. By increasing the demands of OWD but reducing the demands of TUD, the mixed return temperatures that are used to extract heat from the GTD well and the HT-ATES are affected. As OWD has lower return temperatures, the mixed return temperatures are increased, and consequently more thermal energy could be extracted from the heat sources. However, in option 1, the flow is first directed through the evaporator. As the flow through the evaporator increases with higher demands, the temperature difference at the evaporator is reduced. Overall, this results in an unchanged temperature entering the heat exchangers to discharge the GTD well and the HT-ATES in option 1. In option 2, scenario 4 resulted in lower temperatures to extract thermal energy from the HT-ATES. Even though the thermal output extracted from the HT-ATES increased in option 2 and decreased in option 1, the evaluation of the PIs still showed that option 1 performed better than option 2 for the future demand scenario.

Finally, it was analyzed whether the system could be improved by reducing the pump rates of the GTD well and therefore reducing the total power consumption. During medium and peak demands, the flow rate in the GTD well could be decreased if the flow rates in the HT-ATES are increased. As the HT-ATES usually provides lower temperatures than the GTD well, prioritizing the HT-ATES to cover the heat demands requires more heat supply from the WKC or the heat pump to still reach the supply temperature. Therefore, the power consumption of

the GTD well pump was evaluated against the thermal energy supply from the WKC for different flow rates in the GTD well and HT-ATES. How much additional energy is needed from the WKC depends on the hot well temperatures as well as on the required supply temperature in the system. For an exemplary peak demand situation with a supply temperature of 85°C it was shown that changing the merit order and prioritizing the HT-ATES could be feasible for hot well temperatures above 70°C.

Operating the HT-ATES causes an increase of 2450 MWh per year for the GTD well pump to load the HT-ATES compared to the base design. The HT-ATES is loaded continuously over a three-month period with a flow rate of 375 m³/h in the GTD well. An alternative loading strategy was modeled, wherein the flow rate in the GTD well pump was reduced to 260 m³/h and loading of the HT-ATES started in May. This is the lowest possibly flow rate in order to still reach the same volume in the hot well at the beginning of the discharging period in November. A reduction of approximately 7% in the GTD well pump power consumption was achieved. Due to the longer storage time in the hot well, the heat losses were slightly higher and the hot well temperatures dropped faster for a simulation of one full year. As the thermal energy extracted from the HT-ATES was not significantly lower than for the shorter loading strategy, the longer loading strategy is recommended.

4.4 Limitations of the Study

While the model effectively explains the dynamics between the system's components, the exact values presented in the results section will differ from the actual values observed during system operation. Besides the uncertainties associated with any modelling, the results of the model depend highly on the input parameters. For example, the performance of the heat pump will change based on the efficiency of the specific construction model, the chosen working fluid and the size of the heat exchangers.

Some restrictions to the system were neglected in the model. To increase the life expectancy of the GTD well pump, the flow rate can only be adjusted once every 12 hours, based on the expected demands. In the current setup of the model, the flow rate changes on an hourly basis. Also, the system includes several boilers that were simplified as one heat source in the model (WKC). Ramping up these boilers takes some time, whereas in the model heat at any temperature level can be provided by the boilers immediately. Finally, a daily buffer will be added to the system that was not modelled in this study. The buffer will provide thermal energy especially during daily peak demands. Moreover, the aforementioned restrictions make a daily buffer necessary to balance flows and temperatures.

The cut-off temperature of the HT-ATES was set to 61°C in the model throughout the year, which is the average mixed return temperature of TUD and OWD. The exact cut-off temperature changes depending on the flow rates and return temperatures of the consumers. Therefore, the results for the thermal recovery efficiency for the HT-ATES involve a certain degree of uncertainty and could be improved by reducing the cut-off temperature. Besides this, the HT-ATES was modelled assuming an initial temperature and volume at the beginning of a full cycle. However, these values are not known and will vary especially in the first years of operation. The following section presents the results of a simulation over five consecutive years to provide a clearer understanding of the thermal recovery efficiency.

Evolution of the HT-ATES during first years of operation

Figure 41 shows the volume and temperature in the HT-ATES for the first five years of operation for design option 1. As in the previous simulations, the volume and hot well temperature would be the same in design option 2, but the cold well temperatures would be higher. To model the first years of operation, the initial volume is set to zero and the temperatures in both wells start at groundwater temperature. The loading period is set again to three months starting from May every year. It is seen that the volume is unbalanced and therefore increases over the years. After five years, the hot well would have reached a volume of approximately 1.2 million cubic meters. Such a size is problematic, as the hot and cold well would interfere with each other. Also due to other ATES systems on campus, the available space is limited. Furthermore, the volume has to comply with legal limitations of subsurface use. Finally, the smaller the volume of the HT-ATES, the lower is the environmental impact on the subsurface.

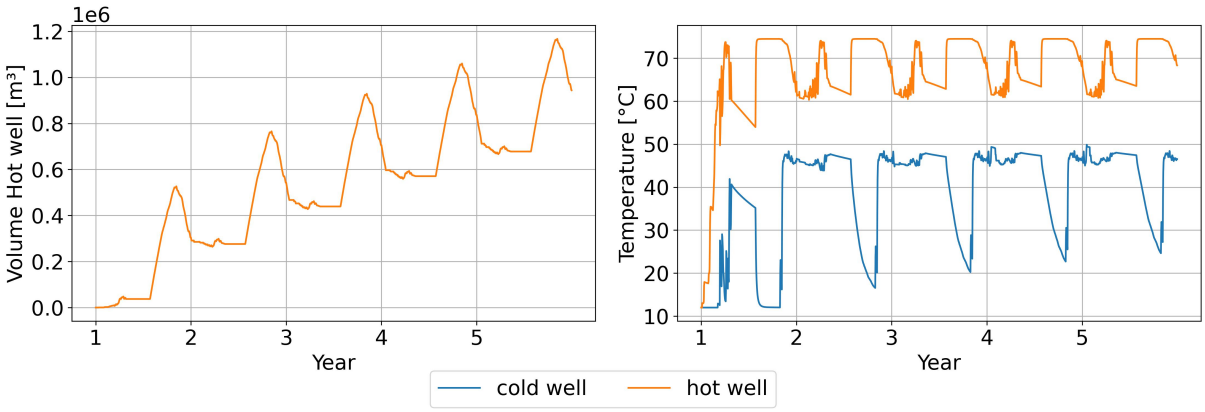

Figure 41 Evolution of the HT-ATES for the first five years of operation (design option 1)

The simulation for five consecutive years also shows how the thermal recovery efficiency of the HT-ATES improves during the first years of operation (Figure 42). For the first year of operation a thermal recovery efficiency of 0.19 can be expected for design option 1. After five years the efficiency has improved to 0.47. The thermal recovery efficiency stabilizes over the years, approaching a constant value. As shown in Figure 41, the temperature curves for the last two years of the simulation are nearly identical. However, the system is unbalanced as more volume is injected than extracted and therefore the thermal recovery efficiency is unlikely to increase above 0.5.

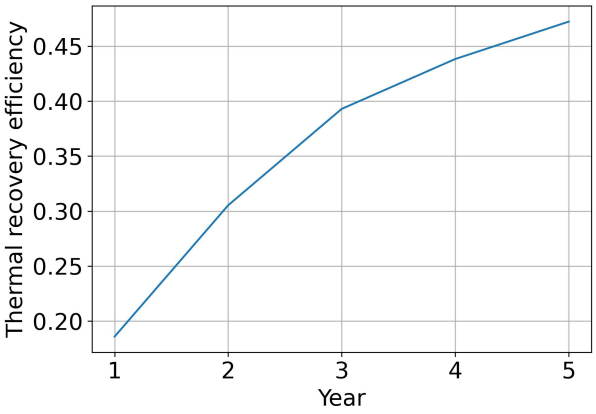

Figure 42 Thermal recovery efficiency of the HT-ATES for the first five years of operation for design option 1

To avoid a constantly increasing volume in the HT-ATES, alternative uses for the warm water that is stored in the hot well but not used in the system have to be found. Alternatively, a limit can be set to the maximum volume in the HT-ATES. Figure 43 shows again the volume and temperature in the HT-ATES for the first five years of operation but with the constraint that the volume cannot exceed 600 000 m³. This limit is based on the assumption that it is the maximum volume for each of the two wells before they begin to interfere with each other. It can be seen that this results in a more balanced system, as injected and extracted volume approach each other. Therefore, the thermal recovery efficiency increases from 0.19 in the first year to 0.54 in the fifth year. Nevertheless, the aquifer still significantly warms up and approximately 450 000 m³ of groundwater at a temperature of 60°C remain unused.

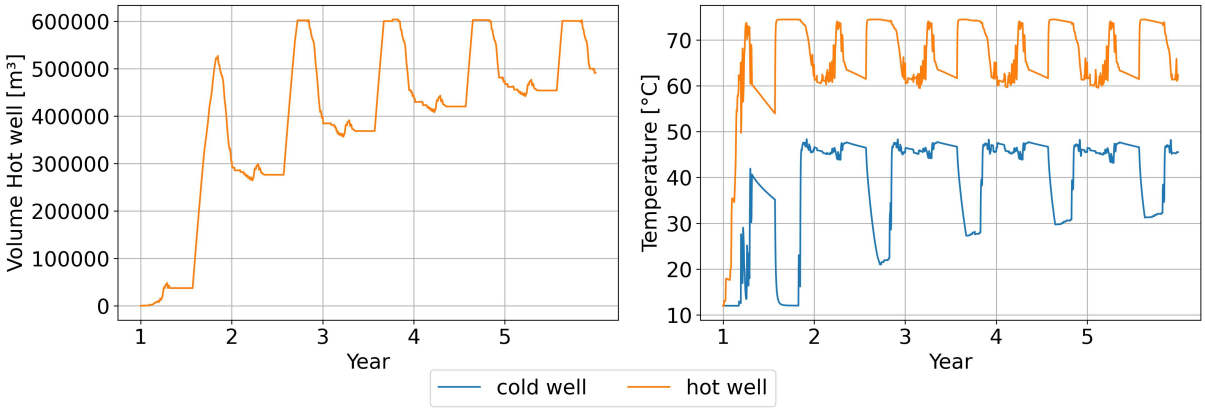

Figure 43 Evolution of the HT-ATES for the first five years of operation under volume constraints (design option 1)

Limiting the volume of the HT-ATES reduces the thermal output that can be supplied from the HT-ATES to the system. Figure 44 compares the annual thermal output of the HT-ATES for an unlimited volume and a volume restricted to 600 000 m³. In the first year of operation, the extracted thermal energy is identical for both scenarios since the volume remains below 600 000 m³. For an unlimited volume, the thermal energy increases every year corresponding to the increasing volume. With a limited volume, the thermal output increases in the second year but once the limit is reached, it decreases every year. As seen in Figure 43, the system is still not fully balanced as more volume is injected than extracted. Therefore, the volume of warm water that cannot be used increases every year and reduces the available space to inject heat from the GTD well.

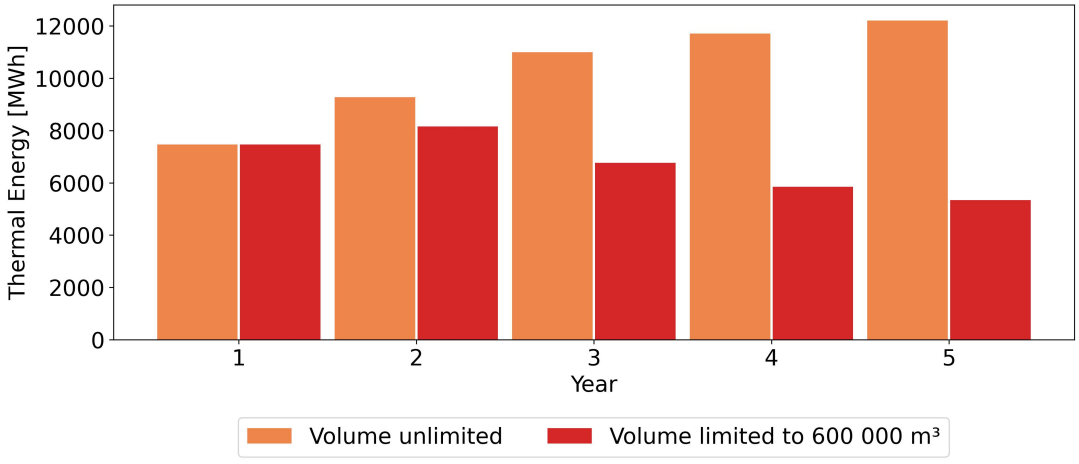

Figure 44 Annual thermal output of the HT-ATES for the first five years of operation (design option 1)

The evaluation of the first five years of operation of the HT-ATES shows that the thermal recovery efficiency of 0.37 (option 1) and 0.19 (option 2) as computed in the results section are representative for the second or third year of operation and might actually improve in the future. On the other side, the computed thermal output of the HT-ATES of approximately 12 000 MWh in design option 1 (see Table 4), can only be reached after five years if no limit is set to the HT-ATES volume. This reveals the need for further considerations on how to limit the volume of the HT-ATES and to identify alternative uses for the warm water that cannot be supplied directly to the system at the end of the discharging period.

5 Conclusion

The aim of this study was to compare different integration options for a HT-ATES into the heating system on TUD's campus based on the evaluation of several PIs. Two design options including an HT-ATES were suggested and compared to a reference design without HT-ATES. The two options differ regarding the location of the HT-ATES within the system. In option 1, the HT-ATES is connected at the outlet of the evaporator. Therefore, the flow used to discharge the hot well is previously cooled down at the evaporator. In option 2, the returning flow from the consumers TUD and OWD is directly used to discharge the hot well without passing the evaporator.

In the evaluation of the system's performance, it was shown that option 1 scored better in all PIs than option 2. As the electricity to operate the system is considered to be supplied from wind and solar energy, the reduction of GHG emissions seems the most decisive PI to evaluate the sustainability of the system. While the heat pump SCOP is useful for comparing different heat pump models, the system SCOP ultimately seems more important for evaluating the overall performance of the system. It includes the thermal energy supply as well as the electricity consumption of the system as a whole and is therefore more representative to evaluate the energy efficiency of the system.

Compared to the reference design, the GHG emissions could be reduced by 31% in option 1 and 29% in option 2. Option 1 also showed the best $SCOP_{HP}$ for the heat pump and the lowest annual electricity consumption of the compressor. However, the annual electricity consumption of the circulation pump in the GTD well is higher in the options with HT-ATES than in the base design due to the loading of the HT-ATES. Therefore, the base design has the best system SCOP. Option 1 still showed a better system SCOP than option 2. Finally, because of the lower temperatures used to extract heat from the hot well, the HT-ATES in option 1 has a better thermal recovery efficiency than in option 2.

Besides a base case scenario, several parameters were adjusted to analyze the robustness of the system. When adjusting supply and return temperature, option 1 still performed better than option 2. For a future demand scenario, in which TUD demands would decrease but OWD demands would increase, the thermal output of the HT-ATES in option 1 was less than in the base case. In option 2, however, the thermal output of the HT-ATES increased for the future demand scenario. Nevertheless, when comparing the performance of both design options, option 1 still scored higher in the PIs than option 2.

Apart from the PIs, the options were compared in terms of financial aspects and environmental impact. It is worth noting that adding the HT-ATES to the system does reduce GHG emissions, but also significantly increases the CAPEX and OPEX of the system compared to the base design without HT-ATES. Furthermore, the HT-ATES represents an intervention in the subsurface that does affect the groundwater ecosystem. The volume and hot well temperature of the HT-ATES is the same in design options 1 and 2, however the cold well temperature is lower in option 1. This can be seen as positive compared to option 2, as the temperature difference to the surrounding groundwater is smaller.

The loading of the HT-ATES requires additional thermal output from the GTD well, which presumably reduces its operational lifetime. Among the two options with HT-ATES, the GTD well production is slightly lower in option 1 and therefore scores better in terms of sustainability of the GTD well. On the other hand, the production of the GTD well is

subsidized. Thus, the HT-ATES will indirectly increase the revenue of the project. Here, option 2 will actually secure higher subsidy than option 1.

In addition to the general research goal of evaluating the different design options, several subgoals were formulated. The findings of this study regarding each subgoal, along with recommendations for further research, are presented below.

Investigate how the integration concept of the HT-ATES within the system influences overall performance.

The two design options that were presented for the integration of a HT-ATES primarily differ in the flow rate directed through the evaporator. It was shown that this difference has an impact on the proportion of heat supply provided by the respective heat sources. Depending on the flow rate at the evaporator side of the heat pump, the temperature entering and leaving the evaporator changes. This in turn influences the temperature levels that are used to extract heat from the GTD well and the HT-ATES.

In this study, only two design options with HT-ATES were compared. More design options could be explored as well as additional configuration options. For example, a second, smaller heat pump could be added to increase the temperatures extracted from the HT-ATES. The model is currently set up mainly based on the flows in the system. Another configuration could be to operate the system based on the temperatures. The flow through the HT-ATES and the GTD well could be adjusted to control the injection temperatures back into the GTD well and the HT-ATES. This would require additional bypasses to comply with mass balance in the system.

A simple configuration of the HT-ATES was modeled where the well screen was set in the first unconfined layer of the aquifer. Further research could explore variations in the HT-ATES model, such as using a screen length that spans the full aquifer thickness. Besides the advantages of HT-ATES, the environmental consequences of such a system are not fully understood at present. Injecting high temperatures to the groundwater may pose a risk of groundwater contamination. Analyzing different well screen lengths to optimize the shape of the HT-ATES can reduce the environmental effects of the system.

Assess the effect of the heat pump size on storage requirement and overall performance.

The size of the heat pump defines the thermal energy that is extracted from the system at the evaporator. The lower the condenser capacity, the lower is the thermal output at the evaporator and the smaller is the temperature difference between the flows entering and leaving the evaporator. As the temperature leaving the evaporator is used to extract heat from the GTD well, the results in this study showed that an increase in heat pump size also leads to an increase in the heat supplied from the GTD well. In option 1, the same applies for the thermal energy extracted from the HT-ATES: the higher the condenser capacity, the more heat can be supplied from the HT-ATES. In option 2, the thermal output of the HT-ATES is independent of the heat pump size. The volume of the HT-ATES does not change with the heat pump size. The storage volume only depends on the total flows in the system and the flow rates that can be used to extract and inject thermal energy.

Analyze the robustness of the system concerning variations in heat demand, supply and return temperatures.

Generally, the results of the model showed that adjusting parameters can have different effects depending on the mode of operation. Low, medium, and peak demands have to be considered separately to understand the impact of modifications in the input parameters.

It was shown that reducing the return temperatures has a bigger effect in reducing GHG emissions in the design options with HT-ATES than in the reference design. This is because lower return temperatures also reduce the cut-off temperature of the HT-ATES. Reducing the supply temperature results in a better $SCOP_{HP}$ in all options and also has the effect that the heat pump can be turned off for low supply temperatures. By increasing the demands, the flow rates in the system also increase. While this means that more flow is available to discharge the HT-ATES, also less flow can be used to load the HT-ATES. Therefore, when increasing the demands, the volume and temperature of the hot well decreased faster and less thermal energy could be supplied by the HT-ATES.

To make the results comparable, the model was run with the same initial volume and temperature in the HT-ATES and with the same time period to load the HT-ATES. However, this led to the result that increased flows in the system mostly reduce the annual thermal output of the HT-ATES because less flow is available to load the HT-ATES, the hot well temperatures drop faster, and the cut-off temperature is reached earlier. The amount of thermal energy that can be extracted from the HT-ATES depends on the combination of volume and temperature in the hot well. If the flows in the system allow for more thermal energy to be extracted from the HT-ATES, the loading period could be adjusted accordingly.

Investigate how changes in the merit order of the heat sources (GTD well and HT-ATES) affect the system.

The heat energy extracted from the GTD well has a temperature level of 74.5°C throughout the year. As the HT-ATES is loaded with thermal energy from the GTD well, the hot well temperature in the HT-ATES is always lower than 74.5°C. If the HT-ATES is prioritized over the GTD well in the merit order, more thermal energy has to be added from the WKC to reach the same supply temperatures. On the other side, the GTD well pump has a significantly higher power consumption than the circulation pump of the HT-ATES as the GTD well is located much deeper than the HT-ATES. When changing the merit order of GTD well and HT-ATES, the power consumption of the GTD well pump and the thermal output of the WKC must be weighed against each other.

For a specific peak demand and supply temperature, it was shown that for hot well temperatures above 70°C, prioritizing the HT-ATES over the GTD well could reduce the total power consumption in the system. However, in order to reduce GHG emissions, the GTD well should always be prioritized as its circulation pump runs on electricity while the WKC relies on gas.

For a more in-depth understanding, the effect of the merit order on the system performance should be analyzed for different supply temperatures and a full year simulation should be analyzed. An optimal operation of the system would involve constantly adjusting the merit order based on the hot well temperature and the supply temperature required in the system. Such a dynamic operation of the system is difficult to implement with the energy system model that was set up using TESPy.

Compare heat losses and pumping costs for different HT-ATES loading strategies.

The flow rate with which the HT-ATES is loaded in summer depends on the flow rate that is set in the GTD well. Two loading strategies for the HT-ATES were compared: a loading period of three months with a flow rate of 375 m³/h in the GTD well and a loading period of approximately 6 months with a flow rate of 260 m³/h in the GTD well. The results showed that by reducing the flow rate in the GTD well, the power consumption of the GTD well pump could be reduced by 7%. The two strategies showed almost no difference in the hot well temperatures of the HT-ATES. Therefore, stretching the loading period of the HT-ATES and reducing the flow rate in the GTD well should be considered.

Besides the pumping costs for loading the HT-ATES, another aspect to consider when operating the HT-ATES is the total volume of the hot and cold well. Due to the cut-off temperature, the HT-ATES is always loaded more than it can be discharged. Consequently, at the end of each storage cycle, a considerable amount of warm water remains in the hot well that cannot be utilized by the system. If no limit is set to the volume, the HT-ATES would grow infinitely and warm up the aquifer. The model was run for five consecutive years with the constraint that the volume of the HT-ATES is limited to 600 000 m³ per well. The results showed that the thermal output of the HT-ATES would decrease over the years as less volume can be loaded into the HT-ATES every year. To maintain a consistent thermal output from the HT-ATES, other ways of exploiting the hot well at lower temperatures have to be found at least to the point where injected and extracted volume are balanced.

6 References

Axelsson, G. (2012). *Sustainable geothermal utilization*. https://www.researchgate.net/profile/gudni-axelsson/publication/267709577_sustainable_geothermal_energy_utilization/links/546dd8940cf2193b94c5d29d/sustainable-geothermal-energy-utilization.pdf

Bell, I. H., Wronski, J., Quoilin, S., & Lemort, V. (2014). Pure and Pseudo-pure Fluid Thermophysical Property Evaluation and the Open-Source Thermophysical Property Library CoolProp. *Industrial & Engineering Chemistry Research*, *53*(6), 2498–2508. https://doi.org/10.1021/ie4033999

Bloemendal, M. (2023). *Piloting Underground Storage of Heat In geoThermal reservoirs PUSH-IT: Design document Co-simulation Delft demo site.*

Bloemendal, M. (2024, July 24). *PySeawATES: ATES simulation environment seawat-python*. https://github.com/martinbloemendal/PySeawATES

Bloemendal, M., & Hartog, N. (2018). Analysis of the impact of storage conditions on the thermal recovery efficiency of low-temperature ATES systems. *Geothermics*, *71*, 306–319. https://doi.org/10.1016/j.geothermics.2017.10.009

Bloemendal, M., Vardon, P. J., Medema, A., Snelleman, S., Marif, K., Beernink, S., van Veldhuizen, F., Pijnenborg, M., Sudintas, G., & van Oort, T. (October 2020). *Feasibility Study HT-ATES at the TU Delft campus.*

Bloemendal, M., Vardon, P. J., Pijnenborg, M., Sudintas, G., Medema, A., Marif, K., Beernink, S., van Veldhuizen, F., Snelleman, S., & van Oort, T. (2021). *A techno-economic evaluation of high temperature thermal aquifer storage (HT-ATES) for use with the geothermal well on the TU Delft campus.* World Geothermal Congress.

Drijver, B., Bakema, G., & Oerlemans, P. (June 2019). *State of the art of HT-ATES in The Netherlands*. http://europeangeothermalcongress.eu/wp-content/uploads/2019/07/289.pdf

European Commission. (2024, January 22). *Progress made in cutting emissions*. https://climate.ec.europa.eu/eu-action/climate-strategies-targets/progress-made-cutting-emissions_en#:~:text=Documentation-,Introduction,total%20%E2%80%9332.5%25%20in%202022.

European Environment Agency. (2023). *Greenhouse gas emissions from energy use in buildings in Europe*. https://www.eea.europa.eu/en/analysis/indicators/greenhouse-gas-emissions-from-energy

Fadel, M., Reinecker, J., Bruss, D., & Moeck, I. (2022). Causes of a premature thermal breakthrough of a hydrothermal project in Germany. *Geothermics*, *105*, 102523. https://doi.org/10.1016/j.geothermics.2022.102523

Fleuchaus, P., Schüppler, S., Godschalk, B., Bakema, G., & Blum, P. (2020). Performance analysis of Aquifer Thermal Energy Storage (ATES). *Renewable Energy*, *146*, 1536–1548. https://doi.org/10.1016/j.renene.2019.07.030

Gao, L., Zhao, J., An, Q., Wang, J., & Liu, X. (2017). A review on system performance studies of aquifer thermal energy storage. *Energy Procedia*, *142*, 3537–3545. https://doi.org/10.1016/j.egypro.2017.12.242

Geothermie Delft. (2024, June 15). https://geothermiedelft.nl/actueel-update-werkzaamheden-week-51-58

Langevin, C. D. (2008). Modeling axisymmetric flow and transport. *Ground Water*, *46*(4), 579–590. https://doi.org/10.1111/j.1745-6584.2008.00445.x

Langevin, C. D., Hughes, J. D., Banta, E., Provost, A., Niswonger, R., & Panday, S. (2017). *MODFLOW 6, the U.S. Geological Survey Modular Hydrologic Model* [Computer software]. U.S. Geological Survey.

Langevin, C. D., Thorne, D. T., Dausman, A. M., Sukop, M. C., & Guo, W. (2008). SEAWAT Version 4: A Computer Program for Simulation of Multi-Species Solute and Heat Transport. *Techniques and Methods*. https://api.semanticscholar.org/CorpusID:140682903

Overstappen. (2024, July 3). *Energy prices in the Netherlands*. https://www.overstappen.nl/energie/compare-energy/energy-prices-netherlands/

PUSH-IT. (2024, June 15). https://www.push-it-thermalstorage.eu/pilots/delft/

Stemmle, R., Blum, P., Schüppler, S., Fleuchaus, P., Limoges, M., Bayer, P., & Menberg, K. (2021). Environmental impacts of aquifer thermal energy storage (ATES). *Renewable and Sustainable Energy Reviews*, *151.* https://doi.org/10.1016/j.rser.2021.111560

Witte, F. (2024, April 30). *TESPy 0.7.4 - Newton's Nature documentation*. https://tespy.readthedocs.io/en/main/index.html#

Witte, F., & Tuschy, I. (2020). TESPy: Thermal Engineering Systems in Python. *Journal of Open Source Software*, *5*(49), 2178. https://doi.org/10.21105/joss.02178

Zwamborn, M. (2021, November 10). *High-temperature aquifer thermal energy storage: Lecture Urban Energy Institute.* KWR. https://filelist.tudelft.nl/Websections/Urban%20Energy/Lectures/Presentatie%20Marette%20Zwamborn%20nov%202021.pdf

7 Appendix

A. Data Preparation

Two separate heat demand datasets for TUD and OWD were available that did not correspond regarding outside air temperatures, days of the week and hour of the day. For example, if the OWD dataset starts with a Monday as the first day of the year, the TUD dataset also has to start with a Monday as there is a correlation between heat demand and weekday.

The OWD dataset represents modeled demands based on reference outside air temperatures. The TUD demands are values from the year 2023. To compute TUD demands matching the OWD dataset, the TUD dataset was first subdivided into 24 groups according to the hours of a day. For each hour of the day a relation between outside air temperature and demand was established by computing the average demands for several intervals of outside air temperature. It was further differentiated between weekends and weekdays. Figure 45 shows for example the average heat demand of TUD at 9 AM depending on the outside air temperature. The demands are higher during the week than on the weekend and decrease with increasing outside air temperatures. In case of missing data for a specific temperature interval, the computed average demands were extrapolated.

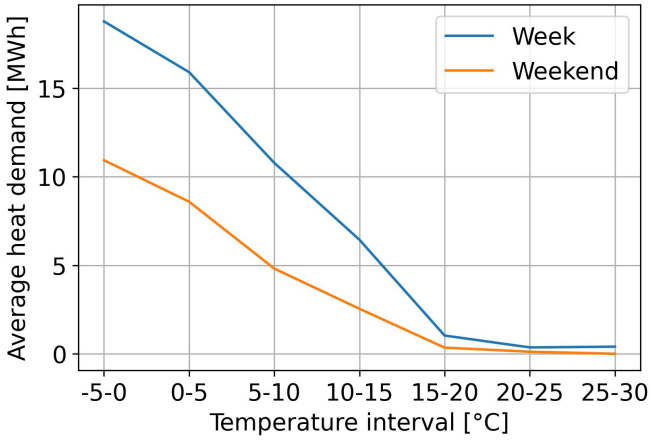

Figure 45 Average heat demand of TUD at 9 AM depending on outside air temperature

In the TUD dataset, the weekdays were included but the OWD dataset didn't have information on the weekdays. To align the two datasets according to their weekdays, an autocorrelation analysis was performed on the OWD dataset to identify if there is a returning pattern showing weekdays and weekends. When looking only at the OWD demands at 8 AM, peaks in the autocorrelation plot can be seen for lags of multiples of 7. This means that there is a correlation between the 8 AM demands of the time series and the 8 AM demands of the same time series 7 days earlier. Figure 46 shows the peaks in the autocorrelation plot highlighted with red circles.

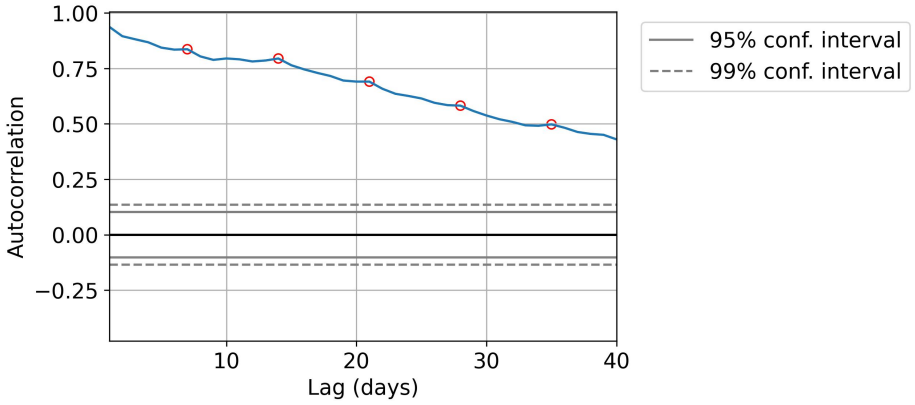

Figure 46 Autocorrelation plot for OWD demands at 8 AM with confidence intervals (dotted line

Figure 47 shows the OWD demands at 8 AM on weekdays and weekends depending on the outside air temperature. During the week, demands are a bit higher at 8 AM than on weekends which corresponds to a peak demand at 8 AM on a regular workday. With this information, weekdays can be assigned to the OWD dataset. Using the average TUD demands of each hour of the day and for specific temperature intervals as established for example in Figure 45, demands for TUD were computed for every entry in the OWD dataset. A complete dataset for the heat demands of TUD and OWD for 8760 hours of a year was obtained.

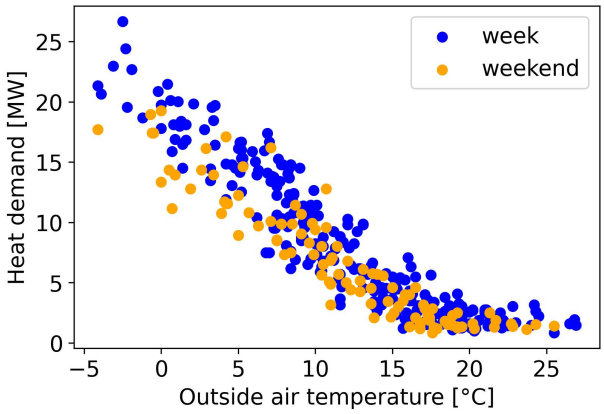

Figure 47 Differentiation of weekdays and weekends demands of OWD (at 8 AM only)

B. Initialization of the HT-ATES

Depending on the duration of the loading and discharging period the volumes and temperatures of the HT-ATES will vary every year. To establish initial values for the model and to be able to compare the different design options, the model was run for one full year starting in May (see Figure 48). If the HT-ATES is loaded whenever possible, the loaded volume exceeds the volume that can be discharged resulting in an unbalanced system. For the heating period from November to April, a volume of approximately 500 000 m³ is needed. Starting with an initial ambient groundwater temperature of 12°C, the hot well quickly heats up to the 74.5°C injected from the GTD well. The cold well only starts to change in temperature when the hot well is discharged in November.

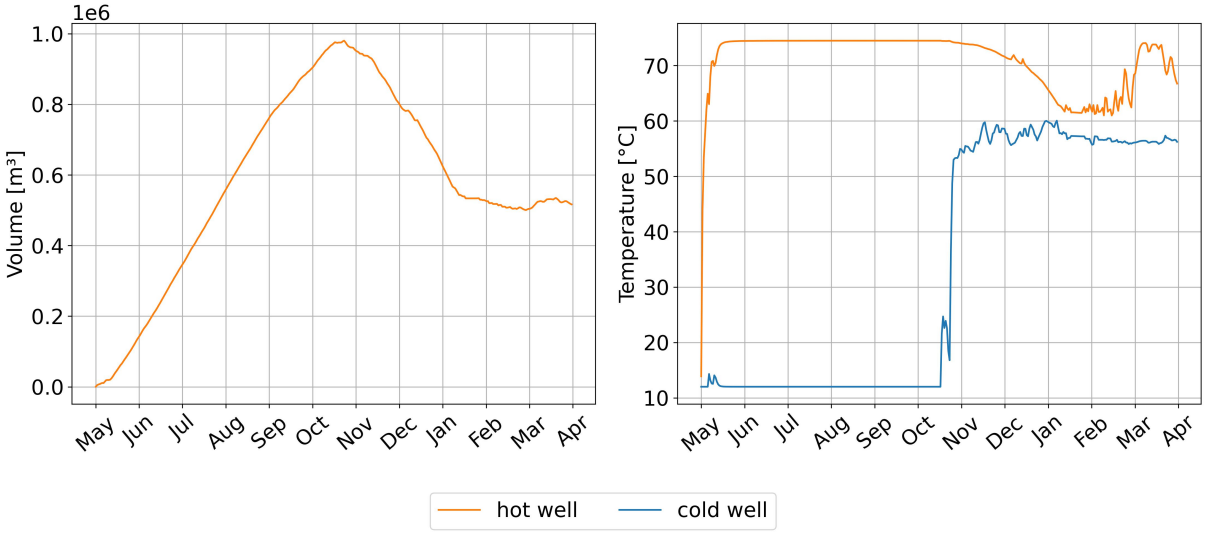

Figure 48 Volume and temperatures of the HT-ATES for first year cycle assuming maximum loading capacity

For the following simulations, the initial volume of the hot well is set to 300 000 m³ in January. The hot well would then be nearly empty at the end of the heating period in April. The initial temperature of the hot well is set to 70°C in January, according to the temperature curve in Figure 48. If the simulation starts in the heating period in January, the temperature of the cold well will immediately increase to the return temperatures of TUD and OWD, so no initial temperature has to be set for the cold well. The loading rate of the hot well volume is almost linear in Figure 48. To reach a volume of 500 000 m³, a loading period of approximately three months is needed, assuming that the HT-ATES is loaded at the maximum flow rate that the GTD well can provide. Therefore, in the following simulations, the HT-ATES is loaded from beginning of August onwards to be fully charged in the beginning of November. In spring, the demands and consequently the flows in the system vary a lot. Therefore, the HT-ATES alters between charging and discharging mode in March and April. This is also maintained in the following simulations, otherwise the temperatures in the HT-ATES would be too low to use from February onwards. From end of April to end of July, the HT-ATES is shut down.

C. Additional Tables and Figures

Table 11 Layer properties used in PySeawATES

Layer	zTop	zBot	Kh	Kv	por	ss	s1	s2	type
1	0	-20	0.05	0.01	0.3	1.00E-05	12	0	aquitard
2	-20	-40	12	2.4	0.3	1.00E-05	12	0	aquifer
3	-40	-45	0.5	0.1	0.3	1.00E-05	12	0	aquitard
4	-45	-50	12	2.4	0.3	1.00E-05	12	0	aquifer
5	-50	-55	0.5	0.1	0.3	1.00E-05	12	0	aquitard
6	-55	-60	12	2.4	0.3	1.00E-05	12	0	aquifer
7	-60	-65	0.5	0.1	0.3	1.00E-05	12	0	aquitard
8	-65	-80	12	2.4	0.3	1.00E-05	12	0	aquifer
9	-80	-100	0.05	0.01	0.3	1.00E-05	12	0	aquitard

Table 12 Performance indicators for the base design depending on condenser size

Performance Indicator	**Condenser size**			
	6 MW	**8 MW**	**10 MW**	**12 MW**
Annual GHG emissions • Q WKC [MWh]	15 277	11 270	8 180	5 839
Annual Electricity consumption				
• W Compressor [MWh]	4 376	5 475	6 410	7 182
• W GTD well pump [MWh]	5 449	5 445	5 441	5 439
SCOP Heat pump [-]	5.10	4.81	4.59	4.42
SCOP System [-]	7.40	6.93	6.57	6.29

Table 13 Performance indicators for design option 2 depending on condenser size

Performance Indicator	**Condenser size**			
	6 MW	**8 MW**	**10 MW**	**12 MW**
Annual GHG emissions • Q WKC [MWh]	11 062	7 965	5 735	4 133
Annual Electricity consumption				
• W Compressor [MWh]	4 060	4 910	5 585	6 109
• W GTD well pump [MWh]	8 030	8 030	8 030	8 030
SCOP Heat pump [-]	5.14	4.88	4.69	4.55
SCOP System [-]	6.40	6.15	5.96	5.81
η_{th} HT-ATES [-]	0.19	0.19	0.19	0.19

Table 14 Performance indicators for the base design for reduced supply temperatures

Performance Indicator	Reduction of Supply Temperature		
	Base Case	**- 2.5°C**	**- 5°C**
Annual GHG emissions • Q WKC [MWh]	11 270	11 025	10 653
Annual Electricity consumption • W Compressor [MWh] • W GTD well pump [MWh]	 5 475 5 445	 4 693 6 063	 4 369 6 153
SCOP Heat pump [-]	4.81	4.77	4.97
SCOP System [-]	6.93	7.12	7.25

Table 15 Performance indicators for design option 2 for reduced supply temperatures

Performance Indicator	Reduction of Supply Temperature		
	Base Case	**- 2.5°C**	**- 5°C**
Annual GHG emissions • Q WKC [MWh]	7 965	8 328	8 587
Annual Electricity consumption • W Compressor [MWh] • W GTD well pump [MWh]	 4 910 8 030	 4 226 8 176	 3 768 7 961
SCOP Heat pump [-]	4.88	4.93	4.96
SCOP System [-]	6.15	6.44	6.47
η_{th} HT-ATES [-]	0.19	0.22	0.21

Table 16 Performance indicators for the base design for reduced return temperatures

Performance Indicator	Reduction of Return Temperature		
	Base Case	**- 2.5°C**	**- 5°C**
Annual GHG emissions • Q WKC [MWh]	11 270	9 749	8 405
Annual Electricity consumption • W Compressor [MWh] • W GTD well pump [MWh]	 5 475 5 445	 5 305 5 095	 5 130 4 786
SCOP Heat pump [-]	4.81	4.61	4.43
SCOP System [-]	6.93	7.44	7.96

Table 17 Performance indicators for design option 2 for reduced return temperatures

Performance Indicator	Reduction of Return Temperature		
	Base Case	**- 2.5°C**	**- 5°C**
Annual GHG emissions • Q WKC [MWh]	7 965	5 982	4 394
Annual Electricity consumption • W Compressor [MWh] • W GTD well pump [MWh]	 4 910 8 030	 4 653 7 932	 4 438 7 860
SCOP Heat pump [-]	4.88	4.70	4.52
SCOP System [-]	6.15	6.51	6.80
η_{th} HT-ATES [-]	0.19	0.19	0.17

Table 18 Performance indicators for the base design for increased demand scenarios

Performance Indicator	Increasing the demands		
	Regular demands (10 MW Condenser)	**+ 50%**	**'Scenario 4'**
Annual GHG emissions • Q WKC [MWh]	8 180	31 686	57 406
Annual Electricity consumption • W Compressor [MWh] • W GTD well pump [MWh]	 6 410 5 441	 9 530 6 745	 10 936 7 998
SCOP Heat pump [-]	4.59	4.40	4.42
SCOP System [-]	6.57	5.99	5.75

Table 19 Performance indicators for design option 2 for increased demand scenarios

Performance Indicator	Increasing the demands		
	Regular demands (10 MW Condenser)	**+ 50%**	**'Scenario 4'**
Annual GHG emissions • Q WKC [MWh]	5 735	28 943	53 582
Annual Electricity consumption • W Compressor [MWh] • W GTD well pump [MWh]	 5 585 8 030	 9 002 8 451	 10 302 9 976
SCOP Heat pump [-]	4.69	4.42	4.41
SCOP System [-]	5.96	5.77	5.58
η_{th} HT-ATES [-]	0.19	0.30	0.38

Figure 49 Thermal recovery efficiency as ratio of extracted to injected thermal energy in HT-ATES

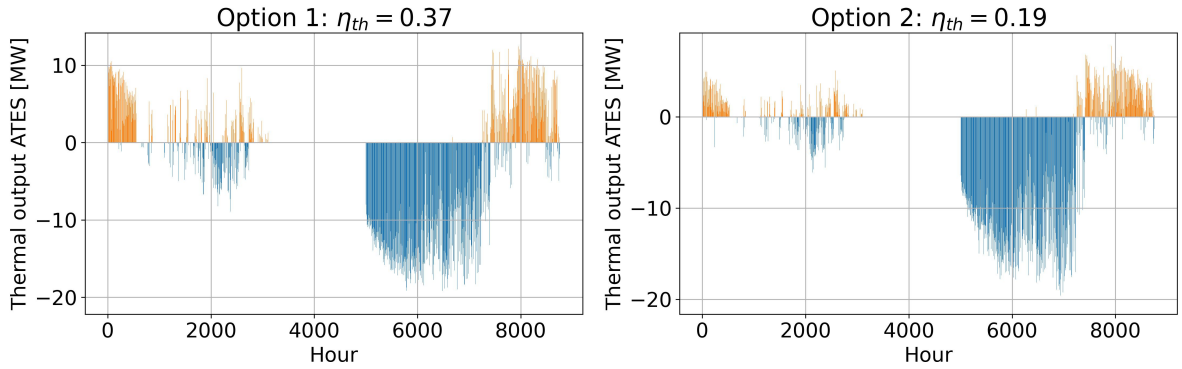

Figure 50 Temperature at the outlet of the evaporator depending on return temperatures (medium demand)

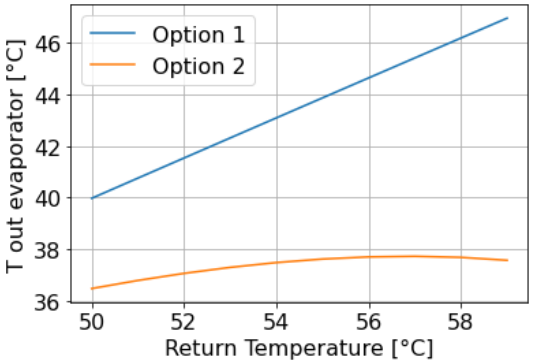

Figure 51 Comparison of hot well temperatures for regular demands and 'scenario 4'